



Ecosystem model optimization using in situ flux observations: benefit of Monte Carlo versus variational schemes and analyses of the year-to-year model performances

D. Santaren^{1,2}, P. Peylin², C. Bacour³, P. Ciais², and B. Longdoz⁴

¹Environmental Physics, Institute of Biogeochemistry and Pollutant Dynamics, ETH Zurich, Universitätstrasse 16, 8092 Zurich, Switzerland

²Laboratoire des Sciences du Climat et de l'Environnement, Commissariat à l'Energie Atomique, L'Orme des Merisiers, 91190 Gif sur Yvette, France

³NOVELTIS, 153, rue du Lac, 31670 Labège, France

⁴INRA, UMR 1137, Ecologie et Ecophysiologie Forestières, Centre de Nancy, 54280 Champenoux, France

Correspondence to: D. Santaren (jean-diego.santaren@env.ethz.ch)

Received: 23 October 2013 – Published in Biogeosciences Discuss.: 20 November 2013

Revised: 28 October 2014 – Accepted: 7 November 2014 – Published: 16 December 2014

Abstract. Terrestrial ecosystem models can provide major insights into the responses of Earth's ecosystems to environmental changes and rising levels of atmospheric CO₂. To achieve this goal, biosphere models need mechanistic formulations of the processes that drive the ecosystem functioning from diurnal to decadal timescales. However, the subsequent complexity of model equations is associated with unknown or poorly calibrated parameters that limit the accuracy of long-term simulations of carbon or water fluxes and their interannual variations. In this study, we develop a data assimilation framework to constrain the parameters of a mechanistic land surface model (ORCHIDEE) with eddy-covariance observations of CO₂ and latent heat fluxes made during the years 2001–2004 at the temperate beech forest site of Hesse, in eastern France.

As a first technical issue, we show that for a complex process-based model such as ORCHIDEE with many (28) parameters to be retrieved, a Monte Carlo approach (genetic algorithm, GA) provides more reliable optimal parameter values than a gradient-based minimization algorithm (variational scheme). The GA allows the global minimum to be found more efficiently, whilst the variational scheme often provides values relative to local minima.

The ORCHIDEE model is then optimized for each year, and for the whole 2001–2004 period. We first find that a reduced (< 10) set of parameters can be tightly constrained by the eddy-covariance observations, with a typical error reduction of 90 %. We then show that including contrasted weather regimes (dry in 2003 and wet in 2002) is necessary to optimize a few specific parameters (like the temperature dependence of the photosynthetic activity).

Furthermore, we find that parameters inverted from 4 years of flux measurements are successful at enhancing the model fit to the data on several timescales (from monthly to interannual), resulting in a typical modeling efficiency of 92 % over the 2001–2004 period (Nash–Sutcliffe coefficient). This suggests that ORCHIDEE is able robustly to predict, after optimization, the fluxes of CO₂ and the latent heat of a specific temperate beech forest (Hesse site). Finally, it is shown that using only 1 year of data does not produce robust enough optimized parameter sets in order to simulate properly the year-to-year flux variability. This emphasizes the need to assimilate data over several years, including contrasted weather regimes, to improve the simulated flux interannual variability.

1 Introduction

In the context of global warming and climate change, the interactions between the terrestrial biosphere and the climate system play a crucial role (Field CB, 2004). Particularly, it is of fundamental importance to assess precisely the distribution and future evolution of terrestrial CO₂ sources and sinks and their controlling mechanisms. To understand and predict CO₂, water and energy exchanges between the vegetation and atmosphere, process-driven land surface models (LSMs) provide insights into the coupling and feedbacks of those fluxes with changes in climate, atmospheric composition and management practices. To achieve this goal, LSMs need finely to describe the processes (i.e., photosynthesis, respiration, evapotranspiration, etc.) that regulate the exchanges between the biosphere and the atmosphere across a wide range of climate and vegetation types and timescales. The level of complexity of LSMs usually encapsulates a description of processes whose timescales range from hours to centuries and whose spatial coverage can spread from flux tower footprints to the global scale.

The equations and parameters of LSMs are usually derived from limited observations on the leaf, soil unit, or plant scales, and are limited to a few plant species, climate regimes, or soil types. Because of the spatial heterogeneity of ecosystems and the nonlinear relationship between parameters and fluxes, difficulties arise in upscaling small-scale process parametrizations and formulations to larger scales, from canopies to ecosystems, regions, and global scales (Field et al., 1995). As a result, major uncertainties remain in modeling the future and global responses of the terrestrial biosphere to changes in the climate and CO₂ (Friedlingstein et al., 2006; Denman et al., 2007).

By fusing observations to model structures, data assimilation methods have shown large potential for improving and constraining biogeochemical models (Wang et al., 2001; Braswell et al., 2005; Trudinger et al., 2007; Santaren et al., 2007; Wang et al., 2009; Williams et al., 2009; Kuppel et al., 2012). Particularly, the time-series measurements from the FLUXNET network provide valuable information on exchanges of CO₂, water and energy across a large range of ecosystems and timescales (Baldocchi et al., 2001; Williams et al., 2009; Wang et al., 2011). At each site out of the 500 sites of this network, fluxes are measured with the eddy-covariance method (Aubinet et al., 1999) on a half-hourly basis and for observation periods that can reach more than 10 years.

Some previous works focused on quantifying how much information could be retrieved from the observations in terms of reducing uncertainties in model parameters. The approach relied on the minimization of a cost function with respect to model parameters. Wang et al. (2001) showed that about three or four parameters of a rather simplified terrestrial model could be estimated independently by assimilating 3 weeks of eddy-covariance measurements of CO₂ and la-

tent, sensible and ground heat fluxes. Braswell et al. (2005) used a 10 year record of half-hourly observations of CO₂ flux to study the influence of data frequencies on inverted parameters. It was shown that parameters related to processes operating on diurnal and seasonal scales (evapotranspiration, photosynthesis) were tightly constrained compared to those related to processes with longer timescales. Santaren et al. (2007) conducted a similar study, but used a complex mechanistic model (ORCHIDEE) with more than 15 parameters to be optimized. In that study, the data assimilation framework was also employed to highlight model structural deficiencies and to improve process understanding.

Performances of parameter optimization schemes have been investigated in several studies (Richardson and Hollinger, 2005; Trudinger et al., 2007; Lasslop et al., 2008; Fox et al., 2009; Ziehn et al., 2012). They could be strongly affected by the way observation errors are prescribed within misfit functions (Richardson and Hollinger, 2005; Trudinger et al., 2007; Lasslop et al., 2008). Contrarily, the choice of the minimizing method amongst an exhaustive panel (locally gradient-based or global random search methods, Kalman filtering) was shown to have smaller influences (Trudinger et al., 2007; Fox et al., 2009; Ziehn et al., 2012). Recently, Ziehn et al. (2012) optimized a simplified version of the process-based BETHY model against atmospheric CO₂ observations. They demonstrated that a gradient-based method (variational approach) manages to locate the global minimum of their inverse problem similarly to a Monte Carlo approach based on a metropolis algorithm, but with computational times several orders of magnitude lower.

Carvalho et al. (2008) challenged the commonly made assumption of carbon cycle steady state at ecosystem level for parameter retrieval, and proposed to optimize parameters describing the distance from equilibrium of soil carbon and biomass carbon pools. More recently, data assimilation implementations have been tested in terms of error propagation, i.e., how information retrieved on optimized parameters influences carbon flux estimation on various timescales (Fox et al., 2009). In those studies, models with a moderate level of complexity were used, and a limited number of parameters was optimized, typically less than 10.

Several studies have shown that calibrating models on a certain timescale does not necessarily imply that predictive skills are improved on all timescales (Hui et al., 2003; Siqueira et al., 2006; Richardson et al., 2007). Particularly, it is important to assess whether the forecast capability of the model could be dampened because of model shortcomings in simulating interannual or long-term processes. One important test of prognostic ability is to assess the model skills in simulating the interannual variability (IAV) of ecosystem carbon fluxes (Hui et al., 2003; Richardson et al., 2007).

The fact that the FLUXNET observations provide information from hourly to interannual timescales allows the investigation of potential time dependencies of parameters, thus highlighting missing processes that should be included

in the models on specific timescales. Reichstein (2003) found that for a rather simple photosynthetic model applied to Mediterranean summer dry ecosystems, parameters should vary seasonally to match observed CO₂ and water fluxes. Similarly, Wang et al. (2007) showed that, for deciduous forests, the photosynthetic parameterization of their model should integrate seasonal variations related to leaf phenology in order to obtain realistic patterns of CO₂, water and energy fluxes. More recently, and in order to search for relationships between carbon fluxes and climate, Groenendijk et al. (2009) optimized a simple vegetation model with only five parameters and investigated the weekly variability of inverted values with respect to different climate regions and vegetation types. Few studies have specifically investigated the equations and parameter generalities across time and spatial scales of complex process-based models. Kuppel et al. (2012) analyzed the ability of a process-based terrestrial biosphere model (ORCHIDEE) to reproduce carbon and water fluxes across an ensemble of FLUXNET sites corresponding to a particular ecosystem (temperate deciduous broadleaf forest), but left apart a detailed study of the model performances across temporal scales.

In this work, we use the same ORCHIDEE model, but we focus on the temporal scale and study the temporal skill of the equations in reproducing seasonal and year-to-year CO₂ and water flux variations at a particular deciduous forest site. To tackle this scientific question, we also investigate in a preliminary step the potential of two different optimization approaches, comparing a gradient-based scheme and a Monte Carlo (genetic algorithm) scheme, to infer the optimal parameters of the process-based model. We use eddy-covariance measurements (daily mean of CO₂ and latent heat fluxes) in a beech forest in France (Hesse) for 4 years (2001–2004) characterized by different weather regimes. More specifically, we investigate the following questions:

- How does a gradient-based method perform compared to a more systematic search of the optimal parameters based on a genetic algorithm (GA)?
- Does the assimilation of 1 year or 4 years of data enhance the model fit to observations equally?
- Are the model equations generic enough to simulate seasonal and year-to-year variations of the CO₂ and water fluxes, and particularly the extreme years (e.g., the summer drought of 2003)?
- Does the information gained from parameter optimization indicate anything new about modeling carbon and water fluxes in deciduous forests?

After a description of the methods (Sect. 2), performances of the gradient-based and GA algorithms are compared (Sect. 3.1). We then optimize the model with daily means of eddy-covariance NEE and water fluxes observed at the

Hesse tower site over the 2001–2004 period. Through cross-validation experiments, we assess the predictive skills of the model when optimized with each different year and with the whole period of data (Sect. 3.2). A posteriori parameter values, errors and correlations are analyzed in order to quantify the contribution of the data assimilation framework in terms of parameter calibration and process understanding (Sect. 3.3). Particularly, we investigate to what extent optimized values may have been biased to compensate for model structural deficiencies. Finally, the temporal skill of the model is studied through its ability to reproduce variations in the NEE from monthly to interannual timescales (Sect. 4.3).

2 Material and methods

2.1 Eddy-covariance flux data

The beech forest of Hesse is located in northeastern France (48° N, 7° E). It is a fenced experimental plot where many studies have been carried out (see the references in Granier et al., 2008). In 2005, it was a nearly homogeneous plantation of 40 year old European beech (*Fagus sylvatica* L.) whose mean height was 16.2 m. Located on a high-fertility site, this young forest, which underwent thinning in 1995, 1999 and at the end of 2004, is growing relatively quickly, and thus acts on an annual basis as a net carbon sink (average NEE equals $-550 \text{ g C m}^{-2} \text{ yr}^{-1}$ over 2001–2004). Long-term mean annual values of temperature and rainfall are, respectively, 8.8 °C and 900 mm.

Fluxes and meteorology are measured in situ and on a 30-min basis by using the standardized CARBO-EUROFLUX protocol (Aubinet et al., 1999). We use hereinafter observations that were made at the HESSE site from 2001 to 2004. Within this period, less than 5 % of the net CO₂ flux (NEE) and latent heat flux (LE) data were missing, and observational gaps mostly occurred during December 2001, February and December 2004, where periods with no data lasted around 10 days. We use original data that were neither corrected for low-turbulence conditions, nor gap filled, nor partitioned (Reichstein et al., 2005; Papale et al., 2006). Data corrections only accounted for inner canopy CO₂ storage.

NEE and to a lesser extent LE fluxes showed high year-to-year variability related to soil water deficit duration and growing season length (Granier et al., 2008). Years 2001 and 2002 were, respectively, moderately dry and wet, whereas 2003 and 2004 were exceptionally dry (respectively, 124 and 100 days of soil water deficit). Moreover, during the summer of 2003 (June to August), mean monthly temperatures were the highest ever observed in this area. Finally, the growing season length (GSL) varied significantly during this period, with an amplitude of 50 days, mostly because of different senescence dates.

2.2 The ORCHIDEE land surface model

The ORCHIDEE (ORganizing Carbon and Hydrology In Dynamic Ecosystems) biogeochemical ecosystem model is a mechanistic land surface model that simulates the exchanges of carbon dioxide, water and heat fluxes within the soil–vegetation system and with the atmosphere; variations in water and carbon pools are predicted variables. Model processes are computed on a wide range of timescales: from 30 min (e.g., photosynthesis, evapotranspiration, etc.) to thousands of years (e.g., passive soil carbon pool decomposition) (Krinner et al., 2005). ORCHIDEE has been applied in a number of site-level (Krinner et al., 2005) and regional CO₂ budget studies forced by climate data (Jung et al., 2007), as well as for future projections of the carbon–climate system, coupled to an atmospheric model (Cadule et al., 2010).

The model contains a biophysical module dealing with photosynthesis and energy balance calculations every 30 min, a carbon dynamics module dealing with the allocation of assimilates, autotrophic respiration components, onset and senescence of foliar development, mortality and soil organic matter decomposition in a daily time step. A complete description of ORCHIDEE can be found in Krinner et al. (2005). The main parameters optimized in this study are defined in Table 1, and the associated model equations are defined in Appendix A. The choice of a subset list amongst the total number of ORCHIDEE parameters is explained in Sect. 2.3.4.

As in most land surface models (LSMs) dealing with biogeochemical processes, the vegetation is described in ORCHIDEE by plant functional types (PFT), with 13 different PFT over the globe. Distinct PFT follow the same set of governing equations, but with different parameter values, except for the calculation of the growing season onset and termination (phenology), which involves PFT-specific equations (Botta et al., 2000). The Hesse forest is described here by a single PFT called “temperate deciduous”, in the absence of understory vegetation at the forest site. Soil fractions of sand, loam and clay are 0.08, 0.698 and 0.222, respectively (Quentin et al., 2001).

In the following, we applied the model in a “grid-point” mode, forced by 30 min gap-filled meteorological measurements made on the top of the flux tower (Krinner et al., 2005). Forcing variables are air temperature, rainfall and snowfall rates, air-specific humidity, wind speed, pressure, and short-wave and longwave incoming radiations.

Biomass and soil carbon pools are initialized to steady-state equilibrium from a spin-up run of the model, i.e., a 5000 year model run using climate forcing data from years 2001 to 2004 repeated in a cyclical way. This ensures an annual net carbon flux close to zero in a multi-year average period. This strong assumption is partly released through the optimization of a scaling factor of the soil carbon pools ($K_{\text{soil C}}$, Eq. A17) to match the observed carbon sink asso-

ciated with this growing forest (see Sect. 4.2 and Carvalhais et al., 2008).

2.3 Parameter optimization procedure

The methodology that we use in this study to optimize the ORCHIDEE parameters relies on a Bayesian framework (Tarantola, 1987): (1) we select a set of parameters to optimize, and a range of variation for each parameter; (2) assuming Gaussian probability density functions (PDF) to describe data and parameter distributions, we define a cost function that embodies a measure of the data–model misfit and prior information on the parameters; (3) we test the performances of a genetic algorithm and a gradient-based one to minimize the cost function, i.e., to locate the optimal parameter set within the parameter space; and (4) we assess errors and correlations in optimized parameters.

2.3.1 Cost function

Assuming that the probability density functions of the errors in measurement, model structure and model parameters are Gaussian, the optimal parameters correspond to the minimum of the cost function $J(\mathbf{x})$ (Tarantola, 1987):

$$J(\mathbf{x}) = (\mathbf{Y} - \mathbf{M}(\mathbf{x}))^t \mathbf{R}^{-1} (\mathbf{Y} - \mathbf{M}(\mathbf{x})) + (\mathbf{x} - \mathbf{x}_p)^t \mathbf{B}^{-1} (\mathbf{x} - \mathbf{x}_p) \quad (1)$$

\mathbf{x} is the vector of parameters to be optimized, \mathbf{x}_p the vector of prior parameter values, \mathbf{Y} is the vector of observations, and $\mathbf{M}(\mathbf{x})$ the vector of model outputs. The error covariance matrices \mathbf{R} and \mathbf{B} describe the prior variances/covariances in observations and parameters, respectively. The first term of $J(\mathbf{x})$ represents the weighted data–model squared deviations (referred to in the text below as J_{OBS} , Sect. 3.2.1). The second term, which is inherent to Bayesian approaches, represents the mismatch between optimized and prior values weighted by the prior uncertainties in parameters (diagonal matrix \mathbf{B} , Table 1). Although we acknowledge that observation and parameter errors do not strictly follow Gaussian distributions, we have used such a hypothesis to simplify the Bayesian optimization problem, which becomes equivalent to a least squares minimization and thus analytically solvable by minimizing a cost function like Eq. (1) (Tarantola, 1987).

The temporal resolution of $\mathbf{M}(\mathbf{x})$ and \mathbf{Y} corresponds to daily averages. We choose daily means in order to assess the ability of the ORCHIDEE model to reproduce observed CO₂ and latent heat flux variability on daily, weekly, seasonal, and interannual timescales, and not the hourly timescale. Because of data gaps, daily means have been calculated only when more than 80 % of the half-hourly data were available.

\mathbf{R} , the data error covariance matrix, should include both data uncertainties (diagonal elements) and their correlations (non-diagonal elements). However, the latter are difficult to assess properly, and we thus neglect them. Data uncertainties (\mathbf{R} diagonal elements) are chosen in such a way that NEE and

Table 1. Parameter names with their description and corresponding model equations (Appendix A), ranges of variation, a priori values and uncertainties of the parameters.

Parameter	Description	Prior	Min	Max	σ_{prior}
Photosynthesis					
$V_{\text{cmax_opt}}$	Maximum carboxylation rate ($\mu\text{mol m}^{-2} \text{s}^{-1}$) (Eq. A5)	55	27	110	33.2
g_{sslope}	Slope of the Ball–Berry relationship between assimilation and stomatal conductance (Eq. A2)	9	0	12	4.8
c_{Topt}	Optimal temperature for photosynthesis ($^{\circ}\text{C}$) (Eq. A11)	26	6	46	16
c_{Tmin}	Minimal critical temperature for photosynthesis ($^{\circ}\text{C}$) (Eq. A9)	−2	−7	3	4
c_{Tmax}	Maximal critical temperature for photosynthesis ($^{\circ}\text{C}$) (Eq. A10)	38	18	58	16
Stomatal response to water availability					
F_{stressh}	Adjust the soil water content threshold beyond which stomata close because of hydric stress (Eq. A6).	6	0.8	10	3.7
K_{wroot}	Root profile that determines the soil water availability (Eq. A7)	0.8	0.2	3	1.12
Phenology					
$K_{\text{pheno_crit}}$	Parameter controlling the start of the growing season (Eq. A30)	1	0.5	2	0.6
c_{Tsen}	Temperature parameter controlling the start of senescence (Eq. A33)	12	2	22	8
LAI_{MAX}	Maximum leaf area index (Eqs. A32 and A31)	5	3	7	1.6
SLA	Specific leaf area (Eq. A28)	0.026	0.013	0.05	0.015
$L_{\text{age_crit}}$	Mean critical leaf lifetime (Eq. A34)	180	80	280	80
K_{LAIhappy}	Multiplicative factor of LAI_{MAX} that determines the threshold value of LAI below which the carbohydrate reserve is used (Eq. A32)	0.5	0.35	0.7	0.14
τ_{leafinit}	Time in days to attain the initial foliage using the carbohydrate reserve (Eq. A31)	10	5	30	10
Respirations					
K_{soilC}	Multiplicative factor of the litter and soil carbon pools (Eq. A17)	1	0.25	4	1.5
Q_{10}	Parameter driving the exponential dependency of the heterotrophic respiration on temperature (Eq. A18)	2	1	3	0.8
$\text{MR}_{\text{offset}}$	Offset of the linear relationship between temperature and maintenance respiration (Eqs. A15 and A14)	1	0.1	2	0.76
MR_{slope}	Slope of the linear relationship between temperature and maintenance respiration (Eqs. A15 and A14)	0.16	0.05	0.48	0.172
K_{GR}	Fraction of biomass allocated to growth respiration (Eq. A16)	0.28	0.1	0.5	0.16
Respirations responses on water availability					
HR_{Ha}	Parameter of the quadratic function determining the moisture control of the heterotrophic resp. (Eq. A20)	−1.1	−2	0	0.8
HR_{Hb}	Parameter of the quadratic function determining the moisture control of the heterotrophic resp. (Eq. A20)	2.4	1.8	6	1.7
HR_{Hc}	Parameter of the quadratic function determining the moisture control of the heterotrophic resp. (Eq. A20)	−0.3	−1	0.5	0.6
HR_{Hmin}	Minimum value of the moisture control factor of the heterotrophic respiration (Eq. A20)	0.25	0.1	0.6	0.2
Z_{decomp}	Scaling depth (m) that determines the effect of soil water on litter decomposition (Eqs. A19 and A21)	0.2	0.05	5	2
$Z_{\text{crit_litter}}$	Scaling depth (m) that determines the litter humidity (Eq. A22)	0.08	0.01	0.5	0.2
Energy balance					
K_{z0}	Rugosity length scaling the aerodynamic resistance of the turbulent transport (Eq. A13)	0.0625	0.02	0.1	0.03
$K_{\text{albedo_veg}}$	Multiplicative parameter of vegetation albedo (Eq. A23)	1	0.8	1.2	0.16
K_{rsoil}	Resistance to the evaporation of the bare soil (Eq. A26)	33×10^3	10×10^3	150×10^3	56×10^3

Table 2. Data errors that are taken into account within the cost function (matrix **R**, Eq. 1). They were determined as the RMSE between a priori model outputs and observations (see text).

Years	2001	2002	2003	2004	2001– 2004 (4Y)
NEE ($\text{gC m}^{-2} \text{ day}^{-1}$)	2	2.5	1.7	1.6	1.9
LE (W m^{-2})	14	12	26.3	20.5	19

LE observations have similar weights in the inversion process; they are defined as the root mean squared error (RMSE) between the prior model and the observations (Table 2). This rather simple formulation leads to relatively large errors (typically 25 % of the maximal amplitude of daily fluxes), which reflects the fact that data uncertainties comprise not only the measurement errors (random and systematic), but also significant model errors (representativeness issues as well as missing processes).

The magnitudes of prior parameter uncertainties (matrix **B**) were chosen (i) according to expert knowledge and (ii) to be relatively large, to minimize the influence of the Bayesian term and thus to provide the maximum leverage of the observations upon the parameters. Moreover, for the minimization algorithms, an additional important information is the range of variation for each parameter; such range is prescribed from expert knowledge and typical observed values (TRY database: <http://www.try-db.org>). As in Kuppel et al. (2012), the prior error for each parameter was thus set to 40 % of its prescribed range of variation (Table 1) and we do not consider correlations between a priori parameter values.

2.3.2 Minimization algorithms

Gradient-based algorithm. Several numerical algorithms can be used to minimize a cost function (Press et al., 1992; Trudinger et al., 2007). In this article, we tested two approaches. The first one, the L-BFGS-B algorithm (Byrd et al., 1995), belongs to the family of gradient-based methods that follow local gradients of the cost function to reach its minimum. It was specifically designed for solving nonlinear optimization problems with the possibility of accounting for bounds on the parameters. The algorithm requires at each iteration the value and the gradient of the cost function with respect to its parameters.

The computation of the gradient can be done straightforwardly and precisely by using the tangent linear model (TL). For complex models, the construction of the TL model is a rather sophisticated operation (even with automatic differentiation tools (Giering et al., 2005)) where threshold-based formulations are not handled and need to be rewritten with sigmoid functions for instance. Alternatively, gradients computations can be approximated with a finite-difference scheme. In this study, we use the TL model of ORCHIDEE, generated by the automatic differentiator tool TAF (Gier-

ing et al., 2005). The computation of the gradient of J with respect to one parameter requires one run of the TL model whose computing cost is about two times a standard run of ORCHIDEE. As the L-BFGS-B algorithm requires around 40 iterations to converge (termination criterion: relative change of the cost function does not exceed 10^{-4} during five iterations) and as we optimize a set of 28 parameters, the total computing time of an optimization is close to 2400 model runs.

Even though the derivatives of $J(\mathbf{x})$ are estimated precisely by the use of TL models, the main drawback of the gradient-based algorithms is that they may end up on local minima instead of locating the global minimum. To assess the importance of this problem, optimizations from different initial parameter guesses have been performed (see Sect. 3.1).

Genetic algorithm. Our second approach to minimizing J is based on a genetic algorithm (GA) that operates a stochastic search over the entire parameter space. The GA was chosen from other global search algorithms (simulated annealing, Monte Carlo Markov chains (MCMC)) because of its ease of implementation and its efficiency in terms of convergence. Particularly, MCMC algorithms were discarded given that their computational expense may be prohibitive with global terrestrial ecosystem models (Ziehn et al., 2012). The GA mimics the principles of genetics and natural selection (Goldberg, 1989; Haupt and Haupt, 2004). When applying a GA for an optimization problem, parameter vectors are considered as chromosomes whose each gene represents a parameter. Every chromosome chr has an associated cost function $J(\text{chr})$ (Eq. 1), which assigns a relative merit to that chromosome. The algorithm starts with the definition of an initial population of n_{chr} chromosomes; each parameter value being randomly chosen within a defined interval (Table 1). Cost functions are then computed for each chromosome. Then, the GA follows a sequence of basic operations to create a new population: (1) Selection of chromosomes from the current population (parents) that will (2) mate and form new chromosomes (children) by exchanging part of their genes (crossover). (3) Additionally, some new chromosomes will come from the mutation of some parents chromosomes. This mutation induces random changes in the parameters (genes) of the parents leading to new chromosomes that are partly independent of the current population. Finally, depending on the user choice, a new generation can be created in several ways: (1) by gathering the current and new populations; (2) by selecting the best chromosomes, i.e., the ones that have the lowest cost function, amongst both populations (elitism); and (3) by integrating the new population only. This new generation is used in the next iteration of the algorithm.

GA performances are sensitive to the way their processes are implemented (selection, recombination or mating, mutation) and to the values of their principal parameters: number of chromosomes n_{chr} , fraction of chromosomes that mate

or mutate, and number of iterations. The best configuration should provide a good balance between, on the one hand, robustness and precision, and, on the other hand, rapidity. In our study, we tested different configurations by optimizing the model against the 2001 Hesse data. The chosen setup of the GA leads on average to the smallest optimal cost function with the smallest number of iterations. For this configuration, the population is of 30 chromosomes and the maximal number of iterations is set to 40. The total computing cost of the GA is hence about 1200 model runs (versus the 2400 model runs of the gradient-based algorithm). Moreover, we set that 80 % of the children chromosomes are created by reproduction processes, and 20 % by mutations. The chromosomes are selected for mating by a roulette wheel process over their cost function values (Goldberg, 1989) and, once two chromosomes have been selected for recombination, they exchange their genes (parameters) by a double crossover point scheme (Haupt and Haupt, 2004). Next generations are then created by selecting the 30 best chromosomes amongst the parents and the children (elitism). This ensures that the population size will be constant.

2.3.3 Posterior uncertainty assessment

Once the minimum of the cost function has been reached by one or the other algorithm – i.e., optimal parameter values have been found – it is crucial to determine which parameters, through the data assimilation system, have been best resolved and which ones have not. Posterior errors and correlations in optimized parameters provide not only an answer to this question, but also the sensitivities of the cost function to each parameter.

If the model is linear with Gaussian distributions for data and initial parameter errors, the posterior probability distribution of the optimized parameters is also Gaussian (Tarantola, 1987). The posterior error covariance matrix \mathbf{P}_a can be directly computed as

$$\mathbf{P}_a = [\mathbf{H}_\infty^t \mathbf{R}^{-1} \mathbf{H}_\infty + \mathbf{B}^{-1}]^{-1}. \quad (2)$$

The matrix \mathbf{H}_∞ represents the derivative of all model outputs with respect to parameters at the minimum of the cost function. Square roots of diagonal terms of \mathbf{P}_a are parameter uncertainties. Large absolute values (close to 1) of correlations derived from \mathbf{P}_a indicate that the observations do not provide independent information to separate a given pair of parameters (Tarantola, 1987).

2.3.4 Optimization settings: parameters to be optimized?

To simplify the problem, we first select among all ORCHIDEE parameters the most significant ones that primarily drive, from synoptic to seasonal timescales, NEE and LE variations. Accordingly, we do not consider, for example, the optimization of soil carbon turnover or tree growth param-

eters that impact the NEE mainly on decadal scales. Finally, we choose a subset of 28 parameters controlling photosynthesis, respirations, phenology, soil water stresses and energy balance (Table 1).

Although only few parameters may be constrained by the observations of NEE and LE, we optimize a large ensemble because it is difficult to assess beforehand parameter sensitivities over the whole parameter space. One drawback may be that the algorithm would give spurious optimized values because of the equifinality problem whereby multiple combinations of parameters yield similar fits to the data (Medlyn et al., 2005; Williams et al., 2009). The analysis of the posterior error covariance matrix (\mathbf{P}_a , Eq. 2) will inform on which parameters are reliably constrained by the observations (Sect. 3.1).

3 Results

3.1 Performances of a gradient-based versus Monte Carlo minimization algorithm

To assess the relative performances of the BFGS and GA algorithms, we designed a twin experiment, using outputs of the model as synthetic data. This model simulation was done for year 2001 with parameters values that were randomly chosen within their permitted range of variation (Table 1). This artificial data set is fully consistent with the model and therefore the optimization of the parameters is not biased by potential model deficiencies or by observations uncertainties. The objective is to assess the accuracy of the optimization algorithms by comparing the assimilated parameters with the “true” ones used to create the synthetic data. Consequently, in order to let the optimization freely recover these parameters, we remove the term of the cost function that restores optimized values to the prior parameter estimates (Eq. 1). We then ran 10 twin optimizations with each algorithm. For the BFGS approach, we started the downhill iterative search from 10 different initial parameters sets that were randomly prescribed within the admissible range of variation of the parameters (Table 1). For the GA, each optimization gives different results, as several of the GA major operations are based on a random generator.

To compare the a posteriori cost functions, we choose to normalize their values by the value of the cost function obtained by running the ORCHIDEE model with its standard parameters. GA shows a much more robust behavior than BFGS insofar as the normalized cost function values for that algorithm range from 0.007 to 0.04 (mean value 0.02, standard deviation 0.01, Fig. 1). In comparison, the BFGS algorithm produces a posteriori cost functions between 0.07 and 0.49 (mean value 0.29, standard deviation 0.14; Fig. 1). Given the complexity of the ORCHIDEE model, the cost function is likely characterized by multiple local minima. These twin experiments thus clearly show that the GA is

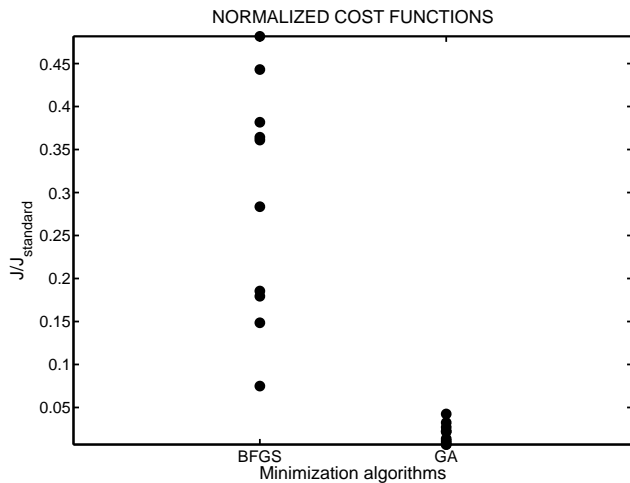


Figure 1. Cost function reductions for the 10 twin experiments that were performed with the BFGS algorithm (BFGS) and with the genetic algorithm (GA). Cost functions (J) at the end of the minimization process were normalized by the value of the cost function representing the mismatch between the synthetic data and the model outputs computed with the standard parameters of ORCHIDEE (J_{standard}).

probably more efficient in minimizing complex cost functions than the BFGS, which is prone, depending on the initial parameter guesses, to falling into local minima. Note that, for our problem, the computing cost of the GA (1200 model runs) is also lower than for the BFGS (2400 model runs).

On average, none of the two algorithms worked well in retrieving the “true” parameter values that were used to generate the synthetic data (Fig. 2). For the best realization of each algorithm, the mean retrieval score across parameters (based on the ratio of the estimated and true values) is about 1, but with a standard deviation of 35 %. Both algorithms likely fail to overcome the equifinality problem; the chosen data assimilation framework and more specifically the type of assimilated data (NEE and LE daily means) do not allow one to distinguish parameters that are correlated (see Sect. 4.2). For most parameters, however, the true values lie in the uncertainty range of the optimized values (1 sigma of the Gaussian PDF), with the error bars crossing the unit horizontal line. Those inverted parameters that show large differences from their a priori values are also characterized by large errors. As Santaren et al. (2007) illustrated for the ORCHIDEE model, the more uncertain an optimized parameter is, the more likely the possibility that the equifinality problem could affect this parameter.

The retrieved parameters that are far from the truth are associated with large posterior error correlations with other parameters, which may explain poor inversion skills. For example, the BFGS optimization did not manage to determine accurately the parameters c_{Topt} , c_{Tmax} , Q_{10} , K_{GR} , HR_{Ha} , HR_{Hb} , HR_{Hc} and K_{rsoil} . Figure 3 shows that the errors on

these parameters are strongly correlated with each others. Besides, these correlations are consistent with the model structure as they concern parameters that are involved in the simulation of the same processes. For instance, HR_{Ha} , HR_{Hb} and HR_{Hc} define the soil humidity control of the heterotrophic respiration (Eq. A20). In summary, we stress again the need to use the information from the posterior variance–covariance matrix, and especially the correlations between parameter errors, to highlight the level of constraint on each parametrization (see Sect. 3.3 with real data).

3.2 Temporal skill of the model equations

The twin experiment results have shown that the genetic algorithm is a more robust method than the gradient-based BFGS algorithm in optimizing the parameters of a model with the complexity of ORCHIDEE. Therefore, we use the GA algorithm to fuse the model with real data collected at the Hesse site.

To address the issue of the temporal skill of the model equations, i.e., their ability to represent year-to-year flux variations, we have designed five cross-validation experiments where the ORCHIDEE parameters are optimized using the Hesse data for different years: 2001, 2002, 2003, and 2004, and for the whole period (2001–2004). The corresponding optimized parameter sets are called X_{2001} , X_{2002} , ..., X_{4Y} . Then, for every five optimized parameter sets, we successively run the model forward and examine the fits to the observations over each year and over 2001–2004. The model runs with X_{2001} , X_{2002} , ... and X_{4Y} are, respectively, called ORC_{2001} , ORC_{2002} , ..., ORC_{4Y} . As expected, the parameter set inverted from observations of a given time period leads to the best model–data agreement during that time period.

Through cross-validation experiments, we investigate how parameters optimized with 1 year or the whole period of observations affect the simulations. More precisely, the optimization against 4 years of observations allows one to estimate if the equations are generic enough to simulate the year-to-year flux variations. Using the 1 year optimized parameter sets to simulate the other years helps to assess the benefit of multi-year versus single-year optimizations. Note that the range of weather conditions during the period 2001–2004 was large, with the wet period in 2001–2002 and the dryer conditions in 2003–2004. This contrast strengthens the analysis of the temporal skill of the model equations.

3.2.1 Cost function reductions

Overall optimization efficiency. For a given time period of assimilated data, the total data–model misfit produced by the resulting optimal parameters is dramatically reduced with respect to the prior one (Fig. 4a). Across the different time periods, the term of the cost function representing the total data–model misfit (J_{OBS} , Eq. 1) is divided by 1 order of magnitude

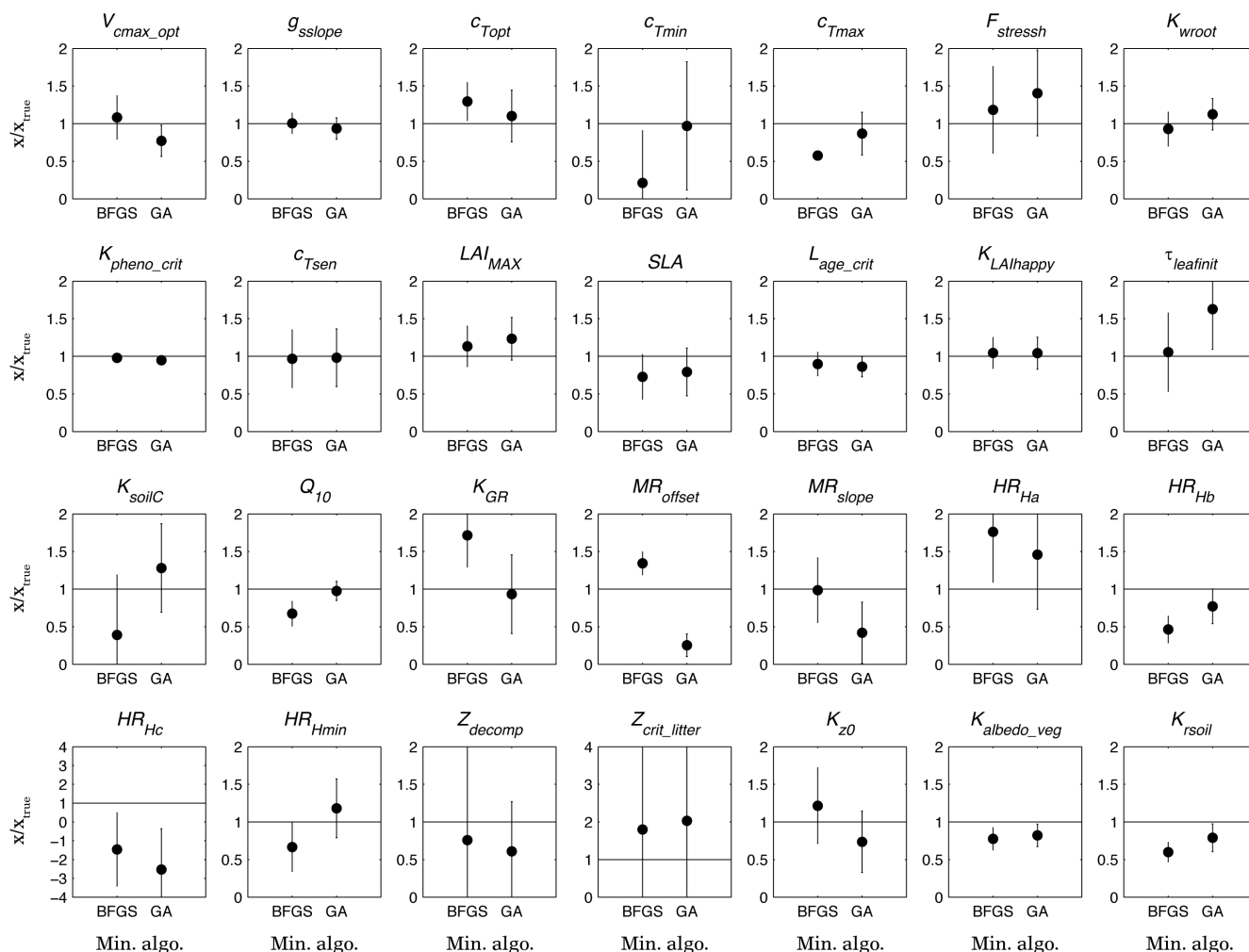


Figure 2. Twin experiments results in terms of parameter inversion. For each parameter, the retrieved values (x) corresponding to the best realization of each minimization algorithm (Min. algo.: BFGS, GA) are divided by the true values (x_{true}) that were used to generate the data so that a value of 1 indicates a perfect retrieval (horizontal lines within the boxes). Along with these values are the a posteriori uncertainties normalized to the true parameter values.

(mean ratio ≈ 0.09 , blue line Fig. 4a) with a standard deviation of 0.04. The different years show different ratios ranging from 0.05 (2002) to 0.14 (2001–2004). These results show that the data assimilation framework has fulfilled its primary target of reducing the total misfit between model outputs and observations. Besides, even though the minimization of the total cost function (Eq. 1) does not make any distinction between types of data, the partial cost functions J_{NEE} and J_{LE} have been reduced by similar amplitudes, respectively, by 88 % and 93 %, with a standard deviation of 4 % for both (green and red lines, Fig. 4a).

Performances of the 4 year optimized parameter set. The 2001–2004 data inversion leads on average to a significant improvement of the fit to the data for each single year of the 2001–2004 period (mean J_{OBS} reduction ≈ 0.16 , Fig. 4f). Even better, the dispersion from year to year of the J_{OBS} re-

ductions is relatively small (≈ 0.04). Hence, the single parameter set X_{4Y} not only enhances the global fit to the 2001–2004 data, but also leads to a significant improvement in the simulation of each single year. These results indicate a substantial predictive ability of the model for periods including wet and very dry summers such as in 2003.

Performances of the 1 year optimized parameter sets. The X_i parameters appear not to be generic enough to enhance in the same proportions the model fit to data of a different year j than the year i of the optimization ($j \neq i$). When using the 1 year inverted parameters to simulate data of a different year, the J_{OBS} cost functions are decreased on average by 68.5 % (mean ratio post/prior J_{OBS} : 0.22 for X_{2001} , 0.4 for X_{2002} , 0.31 for X_{2003} and 0.33 for X_{2004} ; blue line in Figs. 4b, c, d, e). In comparison, these parameters lead on the year used for their optimization to a mean reduction of

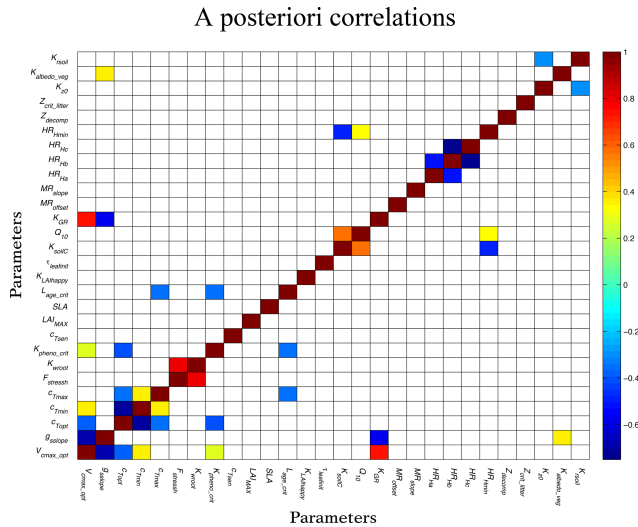


Figure 3. A posteriori correlations between the optimized parameters corresponding to the best twin BFGS optimization. Red and blue squares are, respectively, related to pairs of parameters that are strongly correlated and anticorrelated. White cells correspond to correlations whose absolute values are lower than 0.1.

92 % (ratio post/prior J_{OBS} : 0.13 for X_{2001} on 2001, 0.05 for X_{2002} on 2002, 0.06 for X_{2003} on 2003 and 0.07 for X_{2004} on 2004; Fig. 4a). Likely, the data assimilation framework does not extract enough information from 1 year of data to retrieve robust parameters for simulations in different years. This is particularly true because we have different weather regimes during summer, very dry and hot in 2003 and 2004, normal in 2001 and wet in 2002. The 1 year optimized parameters sets tend to produce reasonable fits for years with similar climates, but much poorer fits for the other years. Over the whole 2001–2004 period, the J_{OBS} reductions are about 79 %, 67 %, 76 % and 75 % for X_{2001} , X_{2002} , X_{2003} and X_{2004} , respectively (mean reduction ≈ 74 %), which is slightly lower than the reduction for the X_{4Y} parameter set (86 %, Fig. 4f).

3.2.2 Fit to the observations

The above analysis of cost function reductions has provided a general and quantitative overview of the performances of the optimized models. Results are now discussed in terms of seasonal fits to NEE and LE.

NEE prior model–data disagreement. The prior model overestimates the magnitude of ecosystem respiration in winter for all years (green curves, Fig. 5). As noticed in Sect. 2.2, carbon pools were initialized from a steady-state spin-up run and the modeled NEE does not represent the current forest carbon uptake (mean NEE = $-550 \text{ g C m}^{-2} \text{ yr}^{-1}$). Also, the prior model does not fully capture the magnitude of the summer uptake period from July to August. ORCHIDEE with prior parameters is however able to reproduce the effect of

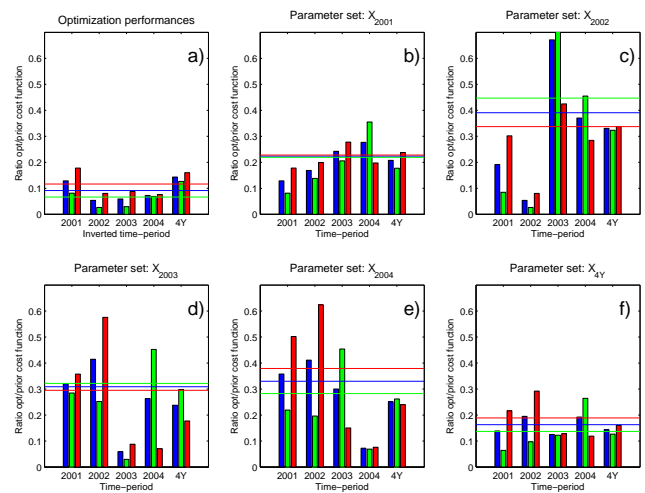


Figure 4. (a) Cost function reductions after optimization of the model against observations of each time period (2001, 2002, ..., 4Y for the whole 2001–2004 time period). Blue bars are associated with the cost function representing the total data–model misfit (J_{OBS} , Eq. (1)); green and red bars are associated with partial cost functions relative to NEE and LE data, respectively (J_{NEE} and J_{LE}). The horizontal lines represent the mean values of the corresponding cost functions reductions. Figures (b), (c), ..., (f) show the cost function reductions produced when running the model with the corresponding optimized parameter sets (X_{2001} , ..., X_{4Y}) in every time period. Horizontal lines are the averaged cost function reductions across other years than the one used to optimize the model.

the strong summer 2003 drought, which causes a positive NEE anomaly (Fig. 5c). Finally, the prior model is unsuccessful in reproducing the beginning and the end of the carbon uptake season during most years but 2003: the starting and finishing dates are on average earlier than 13 days compared to reality.

NEE optimization efficiency. The optimization successfully corrects most of the mismatches described above. For each year, the amplitudes of observed winter release and summer uptake are properly simulated by the model run with the parameter set inverted from that year of observations. The beginning and the end of the carbon uptake seasons are also correctly determined compared to the prior model: after optimization, the mean delay between the model outputs and the observations is decreased to 2.5 days and 2.75 days for the starting and finishing dates, respectively.

Seasonal cycle of the carbon uptake. The 4 year inverted parameter set X_{4Y} leads to a correct simulation of the phase and amplitude of the seasonal cycle of the carbon uptake for most of the years (Figs. 5a, b, c, d). On the contrary, the model run with 1 year optimized parameter sets tends to reproduce the start of the NEE decrease during spring of a different year more incorrectly than the one used for the inversion. A good example of this bias is the model run with X_{2003} , which predicts a NEE decrease much earlier than

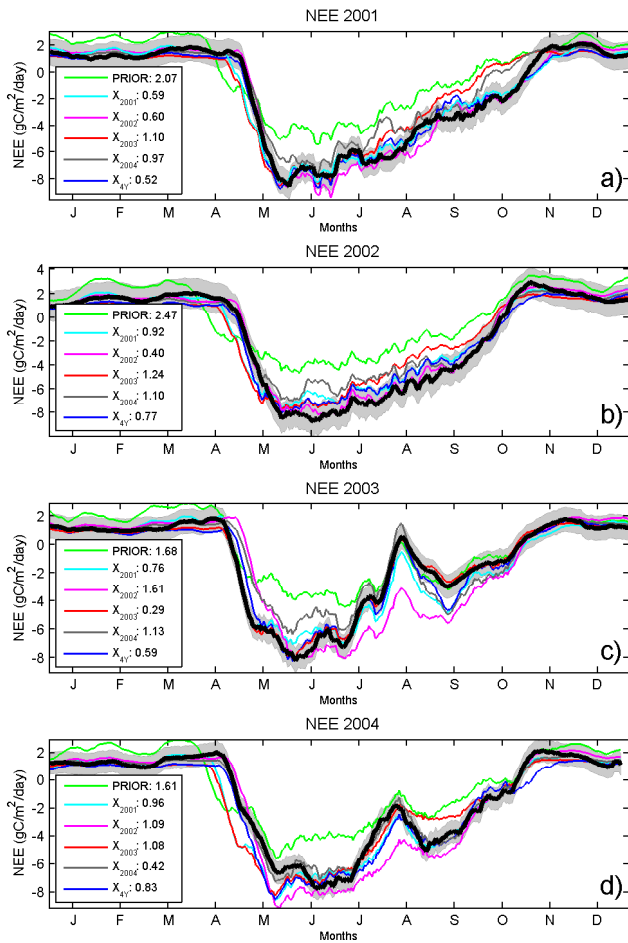


Figure 5. For 2001, 2002, 2003 and 2004, fits to the net CO₂ flux observations (thick black curve) of the model run with the prior and the optimized parameter sets. Figure legends show the model–data RMSE for the different parameter sets. Observation errors are represented by the grey shaded area.

observed for the years 2001, 2002 and 2004 (Figs. 5a, b, d). Probably, the description of leaf onset processes (Botta et al., 2000) is too empirical to allow capturing of year-to-year variations when its associated parameters ($K_{\text{pheno_crit}}$, K_{LAIhappy} and τ_{leafinit}) are optimized with only 1 year of data. Moreover, 1 year optimized models fail to simulate the observed carbon uptake magnitude of a different year. For instance, the model parameterized with X_{2001} , X_{2003} and X_{2004} systematically underestimates the carbon uptake amplitude of the year 2002 (Fig. 5b).

Extreme 2003 summer drought. None of the optimized models but ORC₂₀₀₃ was able to reproduce the amplitude of the abnormally low uptake during September 2003 (Fig. 5c). Most of them (ORC₂₀₀₁, ORC₂₀₀₄ and ORC_{4Y}) reproduce efficiently the effect of the hydric stress and the subsequent sharp drop in CO₂ uptake at the beginning of August, during heat wave conditions, but they overestimate the follow-up recovery of NEE in September. Detailed in situ measurements

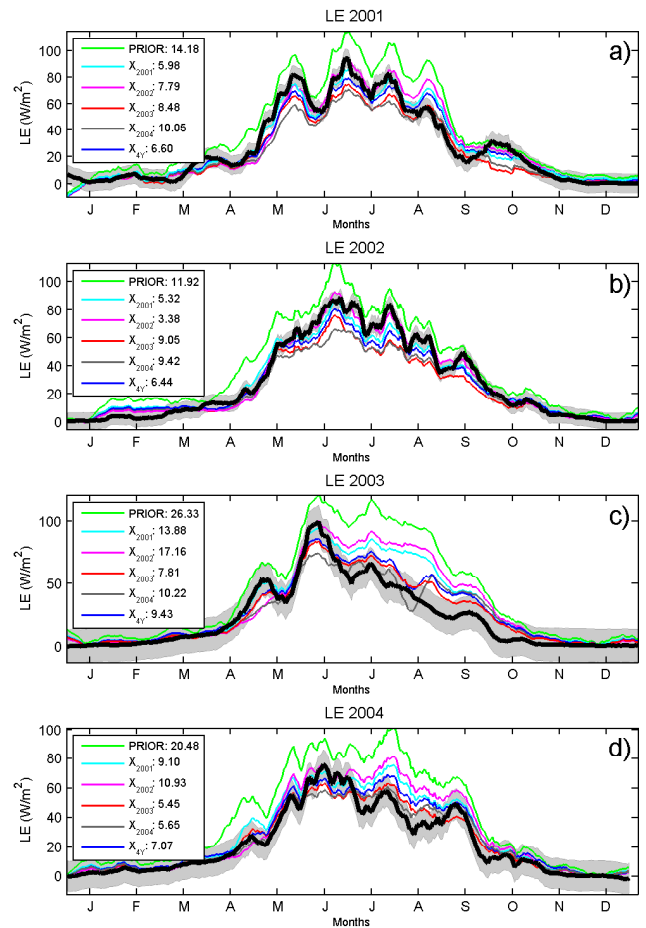


Figure 6. For 2001, 2002, 2003 and 2004, fits to the latent heat flux observations (thick black curve) of the model run with the standard and the optimized parameter sets. Figure legends show the model–data RMSE for the different parameter sets. Observation errors are represented by the grey shaded area.

have led to the conclusion that heavy hydric stress events may damage photosynthetic organs, inhibiting further photosynthetic assimilation, or may cause embolism due to cavitation (Breda et al., 2006). As these physiological behaviors are not modeled by ORCHIDEE, most of the inverted models, except ORC₂₀₀₃, consistently overestimate the gross primary production (GPP) during September 2003. To fit NEE 2003 data, the optimization probably produces misleading values of the X_{2003} parameters (notably c_{Tmax} ; see Sect. 3.3), which in turn explains the poor NEE fit during September 2001, 2002 and 2004 of the ORC₂₀₀₃ model.

LE prior model disagreement with data. For all years, the prior model overestimates the magnitude of the latent heat flux nearly all year long (Figs. 6a–d). This bias is particularly important during summertime periods, and dry years such as 2003 and 2004. The LE bias reaches up to 40 W m⁻² in 2003–2004 compared to 20 W m⁻² in 2001–2002. In addition, prior modeled LE may precede the observation in

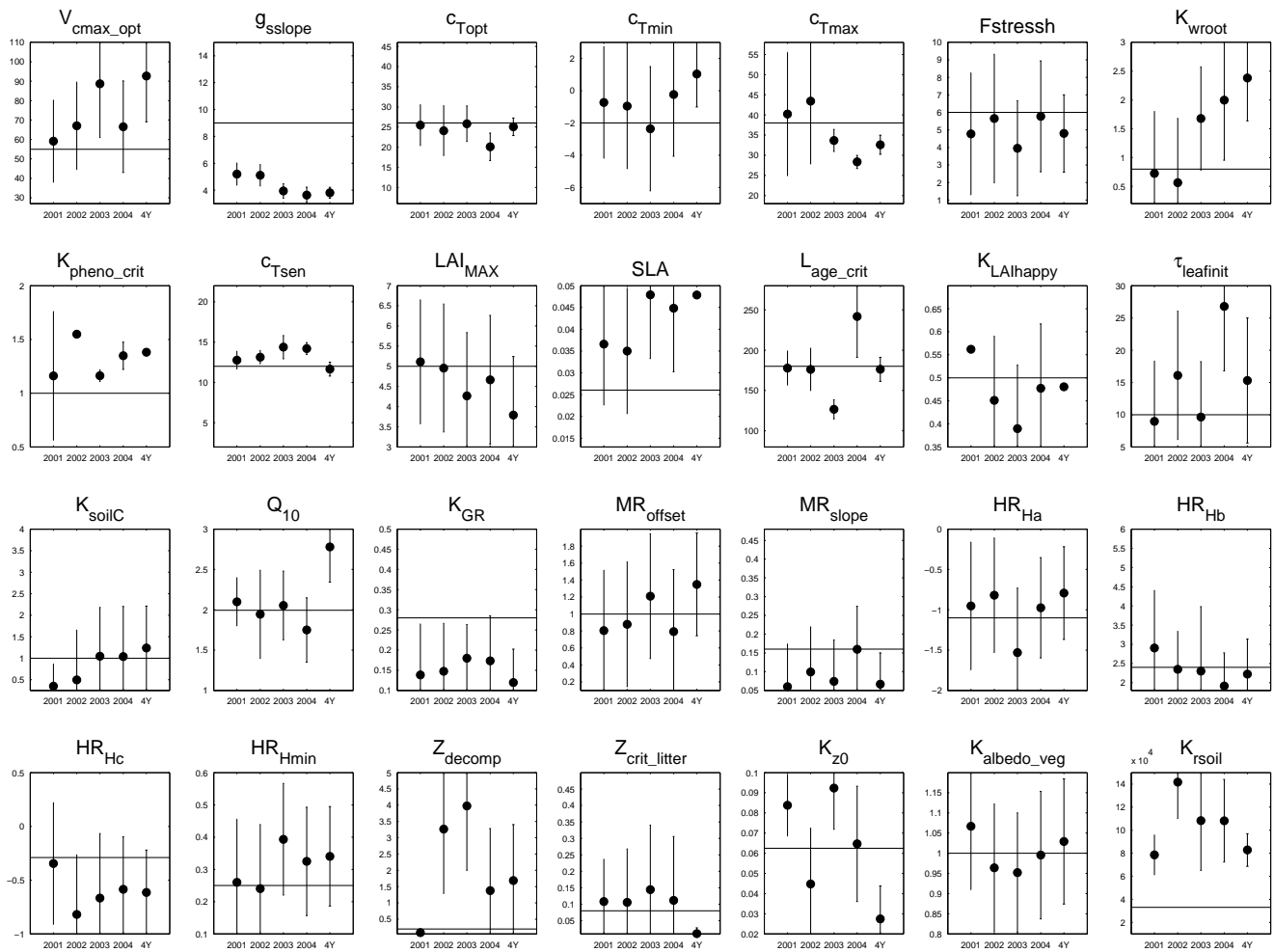


Figure 7. Optimized parameter values (circles) and errors (vertical bars) estimated by the data assimilation system in every time period (2001, 2002, . . . , 4Y for 2001–2004). Box heights specify the ranges within parameters are allowed to vary during the optimization process. Horizontal lines are the a priori values of the parameters.

spring. This phase difference is particularly striking in 2002 and 2004, when canopy evapotranspiration starts much earlier than observed. This could be related to biased parameterization of leafout phenological processes or to a wrong assessment of the transpiration intensity. Also, observations of LE may be underestimated because of the lack of energy closure observed in FLUXNET data (Wilson et al., 2002).

LE optimization efficiency. For each 1 year parameter inversion, the corresponding optimized model reproduces substantially better the LE observations than the prior model for that particular year (Figs. 6a–d). Nevertheless, for each year but 2002, it underestimates both the peak of LE in early June and the subsequent decrease of the transpiration over the summer (Figs. 6a, c and d). Possibly, these deficiencies illustrate structural shortcomings of the model in correctly computing the stomatal conductance and/or the vapor pressure deficit during summer periods, with a “big leaf” approach

(Jarvis P.G., 1995) that does not consider any gradient of humidity from the free atmosphere down to the leaf level.

LE fits of the 4 year optimized model versus the 1 year optimized models. As expected, the inversion using the whole period (X_{4Y} parameters) produces the best compromise throughout the years. Indeed, for a given year of observations, ORC_{4Y} generally outperforms the models inverted from a different year, with the two exceptions of the fits to the LE data of 2002 by ORC_{2001} and 2004 by ORC_{2003} .

3.3 Parameter and uncertainty estimates

Level of constraint on the parameters. Only a few parameters are tightly constrained by the observations if we take as a criterion an error reduction greater than 90% (error reduction \equiv ratio of the *a posteriori* uncertainty to the range of variation). The optimized values of these parameters are characterized by lower relative a posteriori uncertainties than other parameters (Fig. 7). When inverting 4 years

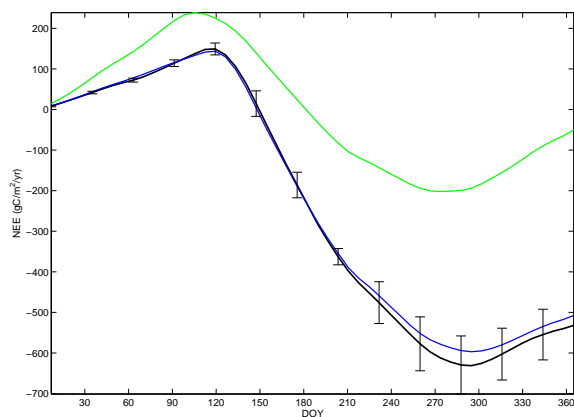


Figure 8. Yearly trend of the cumulative weekly NEE averaged over 2001–2004 for the observations (black curve), for the model run with the a priori parameter set (green curve) and with the 2001–2004 inverted parameter set (X_{4Y} , blue curve).

of observations, nine parameters are determined precisely by the optimization framework: g_{sslope} (stomatal conductance, Eq. A2), c_{Topt} (temperature control of the photosynthesis, Eq. A11), c_{Tmax} (temperature control of the photosynthesis, Eq. A10), K_{pheno_crit} (leaf onset, Eq. A30), c_{Tsen} (temperature control of the senescence, Eq. A33), SLA (specific leaf area, Eq. A28), L_{age_crit} (leaf age driving of the senescence, Eq. A34), $K_{LAIhappy}$ (leaf onset, Eq. A32) and Z_{crit_litter} (litter humidity, Eq. A22). The inversion of 1 year of observations produces a lower constraint on the parameters: only four, three, five and five parameters are precisely determined for the 2001, 2002, 2003 and 2004 optimizations, respectively. Whatever the time period used for the optimization, 18 parameters are weakly constrained by the observations. Note that, contrary to previous studies, the maximum photosynthetic carboxylation rate (V_{cmax_opt} , Eq. A5) is not among the most constrained parameters (Wang et al., 2001, 2007; Santaren et al., 2007).

Hydric stress constraints. The data assimilation framework optimizes processes related to the temperature control of the carbon assimilation to match the observed NEE during hydric stress events. The c_{Tmax} parameter (Eq. A10), the maximal temperature where photosynthesis is possible, is indeed much better constrained in 2003 and 2004 than the parameters related to soil hydric control of the fluxes (K_{wroot} , $F_{stressh}$, HR_{Ha} , HR_{Hb} , HR_{Hc} , HR_{Hmin} , Z_{decomp} and Z_{crit_litter}). Moreover, the retrieved c_{Tmax} values for both periods are lower than a priori. Photosynthesis is suppressed for temperatures warmer than 33 °C in 2003 and 27 °C in 2004. As the soil water stress periods during the summers of 2003 and 2004 are characterized by mean temperatures close to those values, the optimization process likely uses the temperature control of the carbon assimilation to reduce the GPP rather than changing soil water stress functions to match the observed NEE. Whether or not this potential bias is a numer-

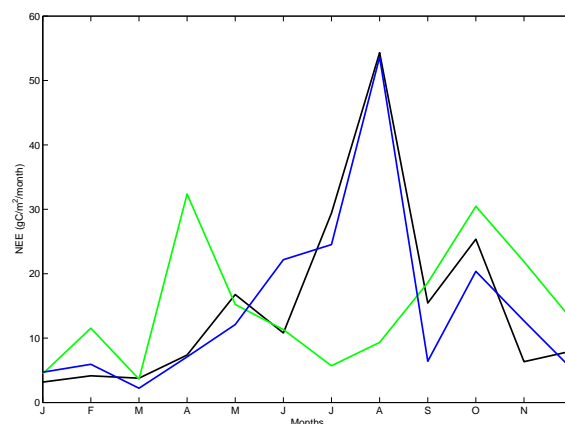


Figure 9. Standard deviations over 2001–2004 of the monthly NEE for the observations (black curve), for the model run with the standard parameter set (green curve), and with the 2001–2004 inverted parameter set (X_{4Y} , blue curve).

ical artefact due to the relative simplicity of the hydrological model (Choisnel, 1977) needs further investigation.

Leaf onset. For all inverted time periods of data, the parameter K_{pheno_crit} (accumulated warming requirement before bud burst; Eq. A30) is tightly constrained, indicating that it plays a major role in the determination of the start of the growing season. The adjustment of the 1 year inverted values are positively correlated with the timing of the leaf onset of the year used in the optimization. Examples are the 2002 and 2003 spring periods, which show, respectively, the latest and earliest starting dates, and lead, respectively, to the largest and smallest optimized values for K_{pheno_crit} . This correspondence is consistent with the phenology description in ORCHIDEE. The smaller the value of K_{pheno_crit} , the earlier the leaf onset will occur (Eq. A30). The 4 year inverted value of K_{pheno_crit} , which is approximately the average of the 1 year optimized values, allows a reasonable fit to the starting dates of the carbon uptake season (Fig. 5). However, further refinement of this approach including a possible modulation of K_{pheno_crit} with past climate can be envisaged.

Poor determination of heterotrophic respiration parameters. Because of error covariances (Fig. 3), some inverted parameters may show very different values amongst the inverted time periods. The Q_{10} parameter, the temperature dependency of the heterotrophic respiration (Eq. A18), is a noticeable example. The X_{4Y} value, $Q_{10} = 2.8$, is much higher than the average value of Q_{10} from all 1 year inversions ($Q_{10} \approx 2$). Error correlation between Q_{10} , K_{soilC} and HR_{Hx} due to the formulation of heterotrophic respiration processes (Eqs. A17, A18 and A20) may explain this feature. Consistently, the parameter K_{soilC} , which scales the sizes of the initial carbon pools (Eq. A17), also shows large variability in its optimized values, depending on the time period used for the inversion. Additional observations, like soil carbon flux/stock measurements, should be assimilated in order to

constrain the heterotrophic respiration parameters better (see Sect. 4.2).

4 Discussion

4.1 Minimization algorithms

From a technical point of view, the goal of parameter optimization is to efficiently and robustly locate the global minimum of a cost function with respect to model parameters. With highly nonlinear and complex models, this task is not straightforward, because cost functions can contain multiple local minima and/or be characterized by irregular shapes. These caveats may prevent gradient-based algorithms from converging to the absolute minimum. In this study, this has been verified insofar as the convergence of a gradient-based method was shown to be very sensitive to first guess parameter values. Note that our experiment considered a relatively large range for the random selection of the first guess point: uniformly distributed over the entire parameter range. We have tested a more restricted range (50 % of the parameter range) and the results, although more consistent with those from the GA, still highlight the convergence problem. When applied to complex models and many parameters, gradient-based methods should then be used with caution, and the search of global minima should be initiated from different starting points in order to get around local minima and potential nonlinearities. Alternatively, we showed the efficiency and robustness of a genetic algorithm (GA) to perform a global random search over the parameter space. The GA appears to be adapted to the optimization of complex models, as it can deal with nonlinearities and is hardly affected by the presence of local minima.

The advantage of using gradient-based methods relies on the possibility of using an adjoint operator to compute the gradient of the cost function. Then, regardless of the number of inverted parameters, the computing cost of the gradient is similar to the one of a forward run of the model (Giering and Kaminski, 1998). Nevertheless, the implementation of an adjoint code is a complicated process even with the use of automatic differentiation tools (Giering et al., 2005). An important programming work is required especially if the model contains parameterizations with thresholds. Moreover, to locate the global minimum without falling into local minima, the minimization process should be still run from different first guesses of the parameters. At the opposite end, the implementation of a GA does not require high informatics skills, even though the settings of this algorithm have to be carefully determined in order to enhance its convergence (see Sect. 2.3.2). Last but not least, GAs can be easily parallelized, which substantially decreases the computing cost and makes it comparable to one of the adjoint techniques.

4.2 Parameter optimization and observations

Although only few parameters may be well constrained by the eddy-covariance flux observations of CO₂ and water (see Sect. 3.3), removing parameters from the optimization process could bias the estimated values of the remaining ones. Also, it is difficult to choose the most sensitive parameters of a model, because the choice depends on the overall model configuration. For example, the ORCHIDEE modeled GPP is sensitive to the maximal temperature for photosynthesis (c_{Tmax} , Eq. A10) during years 2003 and 2004, whereas this parameter has little influence during years 2001 and 2002 (Fig. 7). Finally, even though some parameters may be associated individually with a low sensitivity of the cost function, their combined influence could become important. To illustrate this point, we performed the optimization with a reduced set of parameters that contains the most sensitive parameters as derived from the a posteriori error estimates (see Sect. 3.3): g_{slope} , c_{Topt} , c_{Tmax} , K_{pheno_crit} , c_{Tsen} , L_{age_crit} , SLA , $K_{LAIhappy}$, Z_{crit_litter} , Q_{10} and K_{soilC} . When performing the optimization against the full period, the optimal-to-prior cost function ratio is 0.52 compared to 0.14 for the optimization with the full set of parameters (Sect. 3.2.1). The large deterioration of the optimal fits to the data when using this limited parameter set strengthens the importance to take into account as many uncertain parameters as possible in the optimization process. Ideally, we should optimize all parameters of the model that have a significant uncertainty, but practically it may hamper/slow the convergence of the minimization algorithms and considerably increase the computing cost of the optimizations, we therefore choose a relatively restricted parameter set (see Sect. 2.3.4).

To increase the level of constraint on the carbon cycle parameters, observations of carbon stocks (i.e., mainly above-ground biomass and soil organic matter content) could be used in addition to eddy-covariance flux data. Indeed, flux data provide information on the diurnal to annual timescales of the net carbon exchange, and consequently help to constrain processes on these timescales. Carbon pool data would provide information on longer timescale processes and, even more importantly, would help to separate the contributions from the carbon stock and the rate of decomposition in the computation of respiration fluxes (based on first-order kinetic equations). Our data-assimilation system starts with a prior model that is at equilibrium with the atmosphere, as is commonly done in most global simulations (annual simulated NEE close to zero, see Sect. 2.2), thus with potential biases in the soil and vegetation above-/below-ground carbon pools. This may affect the optimal values of the parameters, even with the use of a parameter that scales the initial soil carbon pools (scaling factor K_{soilC} , Eq. A17). To investigate the impact of the equilibrium state assumption on the estimated parameters related to the temperature and humidity sensitivity responses of the respirations, we perform the 2001–2004 optimization with soil carbon pool sizes

fixed to different values (within a range of 50 % compared to the estimated values from the standard optimization) and the K_{soilC} parameter not being optimized. The optimal values of the parameters related to the temperature sensitivity functions ($c_{T_{\text{min}}}$, $c_{T_{\text{max}}}$, $c_{T_{\text{opt}}}$, Q_{10} , MR_{offset} , MR_{slope} ; see Table 1) and to the humidity response functions (K_{wroot} , F_{stressh} , HR_{Ha} , HR_{Hb} , HR_{Hc} , HR_{Hmin} , Z_{decomp} , $Z_{\text{crit_litter}}$; see Table 1) of both the photosynthetic assimilation and the respirations were found to depend significantly on the initial soil carbon pools. Due to the complexity of ORCHIDEE, the use of flux data only in the optimization likely prevents one from constraining separately parameters related to the environmental responses of the respirations from those related to the carbon stocks themselves. The use of soil and vegetation above-ground biomass data would help to differentiate these parameters, and it would dampen the influence of bringing the model to steady state. Our choice of optimizing K_{soilC} (scalar to the initial soil C pools) should be considered a compromise, while for the vegetation stocks, we would need to account for the true forest age in the simulation (study in preparation).

4.3 Parameter optimization and model validation

Data assimilation is a valuable method for assessing whether models diverge from observations because of structural deficiencies or because of inadequate tuning of their parameters. If a model is not able to fit the data (within their uncertainties) after a formal optimization of its parameters, its structure and equations should be questioned. In this context, the comparison of model outputs versus data for different weather conditions and different timescales provides valuable information. For example, the analysis of LE daily mean time series highlighted the inability of the model to reproduce completely the large decrease in evapotranspiration flux during dry periods (Fig. 6).

In this study, we have optimized the parameters of ORCHIDEE with NEE and LE fluxes for four 1 year periods and the full 4 year period. With the 1 year inverted parameters, we used the “remaining years” to cross validate the optimization and provide hints of the temporal generality of the equations and the ability of the model to simulate year-to-year flux variations (especially during the extremely warm 2003 summer). For instance, models optimized using one given year of data were able to simulate accurately the beginning of the growing season during that year, although they produce significant shifts in the date of the leaf onset for a different year (Fig. 5). This point highlights the limits of the climate-driven phenology model implemented within ORCHIDEE (Botta et al., 2000). Note that the use of very different weather conditions helps in assessing model structural shortcomings, as illustrated by the fit of the 2003 hydric stress event, where the optimization may compensate for model limitations in simulating drought impacts by overtuning some parameters ($c_{T_{\text{max}}}$), which could limit model performances in a differ-

ent year (Sects. 3.2.2 and 3.3). This model drawback would have been hidden when optimizing against observations of wet years only, which emphasizes the need to consider different weather conditions in any parameter optimization.

Despite model shortcomings, the equations of ORCHIDEE are generic enough to allow the optimization procedure using 4 years of observations to greatly enhance the fit to the NEE/LE data over the whole period (Sect. 3.2.1). To evaluate the performances of the 4 year inverted model further, the optimization results are analyzed for different timescales (seasonal, annual and interannual). We first computed, for each year of the 2001–2004 period, the weekly NEE values in order to remove the synoptic variations. Then, the yearly trend of the cumulative weekly NEE averaged over the 4 years shows to what extent the optimized model reproduces the mean seasonal cycle and the mean annual value of NEE (Fig. 8). In addition, we use the standard deviations of monthly NEE over the 4 year period as a measure of the interannual variation (IAV) of the monthly NEE (Fig. 9). The 4 year optimized model, ORC_{4Y} , simulates fairly well the mean seasonal cycle of the observations, with a slight underestimation of the cumulated NEE in the fall season (maximal difference of $40 \text{ g C m}^{-2} \text{ yr}^{-1}$ on DOY 295, Fig. 8). The mean annual carbon uptake observed in the ecosystem ($531 \pm 64 \text{ g C m}^{-2} \text{ yr}^{-1}$, Fig. 8) is also well captured by ORC_{4Y} ($508 \pm 130.7 \text{ g C m}^{-2} \text{ yr}^{-1}$, Fig. 8), but with a simulated IAV ($130.7 \text{ g C m}^{-2} \text{ yr}^{-1}$) that is almost twice the observed one ($64 \text{ g C m}^{-2} \text{ yr}^{-1}$). Nevertheless, along the year, ORC_{4Y} is able to reproduce the temporal pattern of the observed monthly IAV, except at the beginning (June) and the end (September) of the growing season (Fig. 9), when differences can reach $12 \text{ g C m}^{-2} \text{ /month}$. Note that the prior model was not able to capture the IAV during the peak of the growing season (July, August) and that the optimization drastically improves this feature. Overall, the inversion of daily means across the 4 years leads to a strong enhancement of the model fit to the NEE data on each analyzed timescale, with the exception of the IAV of the annual carbon uptake.

Compared to the case of the 4 year inversion, the model run with parameters optimized with 1 year of observations shows a lower skill when simulating data of the whole period and a much lower skill when applied to specific years with different weather conditions (Sect. 3.2.1). A single year of observation does not likely contain sufficient information to constrain the parameters of ORCHIDEE efficiently. We first showed that fewer parameters are constrained in the 1 year optimizations compared to the 4 year one (Sect. 3.3). Secondly, 1 year optimizations are more prone to producing optimal values that are weakly portable to a time period characterized by different weather conditions (i.e., the phenology with the $K_{\text{pheno_crit}}$ parameter), which may reflect overfitting to compensate for model structural errors.

This work shows the potential skills of ORCHIDEE in simulating on several timescales (from monthly to interannual) the CO_2 and water fluxes of a given beech forest (Hesse

site). Kuppel et al. (2012) led a complementary study on the ability of the same model to represent the ecosystem's diversity within the same plant functional type (PFT; temperate deciduous broadleaf forests); they assessed the potential of the model to simulate, with a single set of optimized parameters, the carbon and water fluxes at 12 sites of the same PFT. Particularly, they have shown that the multi-site optimization leads to model–data RMSE reductions at each site comparable to those of the corresponding single-site optimizations.

5 Conclusions

In this study, we demonstrate that the fit to NEE and LE flux data of a complex terrestrial model like ORCHIDEE can be dramatically enhanced with a Bayesian parameter calibration based on a genetic algorithm (GA). The enhanced robustness of this Monte Carlo approach compared to a variational approach using the gradient of the cost function (BFGS), highlighted in this study at one specific FLUXNET site, calls for further investigation. First, one should verify if the better performance of the GA holds at other sites with different plant functional types. Secondly and more importantly the use of multiple sites in the cost function, as in Kuppel et al. (2012), may “smooth” the shape of the cost function, allowing the retrieval of the global minimum of the cost function more easily with a variational approach than for a single site, possibly outperforming the performances of the GA. These technical questions are beyond the scope of this paper and currently under investigation.

For a multi-year simulation of contrasted weather regimes, the ORCHIDEE model appears to be robust enough to simulate the carbon and water fluxes, with parameters optimized against 4 years of observations. At the opposite end, parameters obtained with the inversion of only 1 year of data do not guarantee the simulation of the year-to-year variability of the NEE and LE fluxes, especially the drought event impact or the timing of the carbon uptake season. This study complements a recent study with the same model, by Kuppel et al. (2012), investigating the generality of the model across different FluxNet sites of the same plant functional type. They showed the benefit of including multi-site data to optimize the ORCHIDEE model, but did not focus on the temporal skill of the model. In this study, we highlight the fact that using at least a few years of contrasted weather regimes is crucial to calibrating the sensitivity of photosynthesis to temperature or soil water stress.

A following step in assessing the predictive ability of the model would be to study the propagation of the estimated parameter errors in the fluxes (Fox et al., 2009; Spadavecchia et al., 2011). This should allow one to distinguish model deficiencies from uncertainties due to parameterization. To constrain the latter better, additional types of data should also be integrated within the optimization. Observations of soil carbon content, respiratory fluxes from flux chamber measurement, above-ground annual wood increment or LAI would help the optimization framework to determine more accurately parameters related to annual or interannual timescale processes.

Appendix A: ORCHIDEE model equations

Hereinafter, we briefly describe the main equations of the ORCHIDEE model involved in the optimization process. Optimized parameters are in bold. Prior values and the allowable range of optimization are summarized in Table 1. An extensive description of the model can be found in Krinner et al. (2005).

Net ecosystem exchange (NEE)

The net ecosystem exchange (NEE) flux is calculated as the sum of four terms:

$$\text{NEE} = \text{MR} + \text{GR} + \text{HR} - A \quad (\text{A1})$$

MR is the maintenance respiration, GR the growth respiration, HR the heterotrophic respiration and A the net carbon assimilation rate (A = photosynthesis minus leaf respiration in light). ORCHIDEE is a “big leaf” model that maps the processes and properties of a whole canopy onto a single representative leaf (Jarvis P.G., 1995).

Photosynthesis

Net assimilation (A), stomatal conductance (g_s) and the CO_2 concentration in the chloroplast are solutions of the following system of three equations:

$$g_s = \frac{g_{\text{slope}}(\text{PFT}) \times w_l \times A \times h_r}{C_a} + g_{\text{offset}} \quad (\text{A2})$$

$$A = V_{\text{cmax}} \times \min(V_r, V_j) \times \left(1 - \frac{\Gamma_i}{C_i}\right) - R_d \quad (\text{A3})$$

$$A = g_s \times (C_a - C_i) \quad (\text{A4})$$

Equation A2 gives the stomatal conductance $g_s(A, C_i)$ following the experimental data of Ball et al. (1987) obtained for plants under no-stress conditions. g_{slope} is the slope of the stomatal conductance versus the A linear relationship, h_r the relative air humidity (%) and C_a the CO_2 atmospheric concentration. g_{offset} is an offsetting parameter (=0.01).

Equation (A3) describes $A(C_i)$ with distinct rates of carboxylation for the Rubisco (RuBP) limited regime (V_r) and the electron transfer limited regime (V_j), following Farquhar et al. (1980) for C3 photosynthesis and Collatz et al. (1992) for C4 photosynthesis.

$V_{\text{cmax}}(\text{PFT})$ is the maximum carboxylation rate when plants are not RuBP neither light limited. It is in turn scaled by several limiting functions depending on soil water availability (f_{water}), leaf age (f_{leafage}) and temperature (f_{temp}):

$$V_{\text{cmax}} = V_{\text{cmax_opt}}(\text{PFT}) \times f_{\text{water}} \times f_{\text{temp}} \times f_{\text{leafage}} \quad (\text{A5})$$

$V_{\text{cmax_opt}}(\text{PFT})$ is the maximum carboxylation rate when any limitation occurs. The dependence factor on soil water availability is function of the water fraction available for the plant

in the root zone f_{wroot} :

$$f_{\text{water}} = \frac{2}{1 + \exp(-F_{\text{stressh}}(\text{PFT}) \times f_{\text{wroot}})} - 1 \quad (\text{A6})$$

Parameter $F_{\text{stressh}}(\text{PFT})$ defines the soil water fraction above which maximum opening of the stomata occurs ($w_l = 1$).

f_{wroot} is described by an exponential root profile along the soil depth Z_{soil} , parametrized by $K_{\text{wroot}}(\text{PFT})$:

$$f_{\text{wroot}} = x_{\text{top}} \exp(-K_{\text{wroot}}(\text{PFT}) \times Z_{\text{soil}} \times a_{\text{top}}) + (1 - x_{\text{top}}) \exp(-K_{\text{wroot}}(\text{PFT}) \times Z_{\text{soil}} \times a_{\text{deep}}) \quad (\text{A7})$$

where x_{top} , a_{top} and a_{deep} are normalized coefficients related to the wetness of the top soil water reservoir and the dry fraction of the top/deep soil water reservoirs, respectively. The soil hydrology is computed following the double bucket model (Choisnel, 1977).

The temperature dependence factor of the maximum carboxylation rate f_w makes the photosynthesis maximal at the temperature T_{opt} and cancels it above T_{max} and below T_{min} :

$$f_{\text{temp}} = \frac{(T_{\text{air}} - T_{\text{min}})(T_{\text{air}} - T_{\text{max}})}{(T_{\text{air}} - T_{\text{min}})(T_{\text{air}} - T_{\text{max}}) - (T_{\text{air}} - T_{\text{opt}})^2} \quad (\text{A8})$$

T_{min} , T_{max} and T_{opt} are quadratic functions of the mean annual temperature T_l :

$$T_{\text{min}} = c_{T_{\text{min}}} + b_{T_{\text{min}}} T_l + a_{T_{\text{min}}} T_l^2 \quad (\text{A9})$$

$$T_{\text{max}} = c_{T_{\text{max}}} + b_{T_{\text{max}}} T_l + a_{T_{\text{max}}} T_l^2 \quad (\text{A10})$$

$$T_{\text{opt}} = c_{T_{\text{opt}}} + b_{T_{\text{opt}}} T_l + a_{T_{\text{opt}}} T_l^2 \quad (\text{A11})$$

where a_{T_i} , b_{T_i} and c_{T_i} are constant coefficients.

The relative leaf efficiency f_{leafage} decreases the maximum carboxylation rate with leaf age. Its shape, shown in Fig. A1 in Krinner et al. (2005), is determined by the prescribed mean leaf lifetime $L_{\text{age_crit}}$.

Equation (A4) calculates the gas phase molecular diffusion of CO_2 from canopy air to chloroplast. Altogether, the system of Eqs. (A2, A3 and A4) is solved iteratively to update at each time step the values of A , g_s and C_i at the leaf level.

To scale up to the canopy level, we integrate the values of A and g_s over the canopy depth, that is, over the leaf area index (LAI), assuming an exponential decrease in the effective maximal carboxylation rate (Johnson and Thornley, 1985) and the light intensity (Beer–Lambert law). Particularly, ORCHIDEE computes a total effective stomatal conductance g_c for the whole canopy:

$$g_c = \int_{l=0}^{l=\text{LAI}} g_s(l) dl. \quad (\text{A12})$$

Aerodynamic resistance (r_a)

The aerodynamic resistance, r_a , describes the resistance to the transfer of matter (CO_2 , Water) and energy between the

canopy and the measurement plane:

$$r_a = \frac{1}{V_{\text{wind}} \times C_d(K_{z0})} \quad (\text{A13})$$

V_{wind} is the windspeed norm. The influence of canopy turbulence and surface roughness is embodied by the surface drag coefficient C_d whose computation depends on a characteristic rugosity length K_{z0} (Ducoudré et al., 1993).

Maintenance respiration (MR)

The maintenance respiration is function of the size of each living biomass pool B_i , and has a linear temperature dependency on the pool (soil or surface) temperature (T_i) (Ruimy et al., 1996). For leaf maintenance respiration, a function of the leaf area index (LAI) also enters the calculation.

$$\text{MR}_{\text{leaf}} = \max(0, C_{0,\text{leaf}}(\text{MR}_{\text{slope}} \times T_i + \text{MR}_{\text{offset}})) \quad (\text{A14})$$

$$\times B_{\text{leaf}}^{\frac{0.3\text{LAI}+1.4(1-\exp(-0.5\text{LAI}))}{\text{LAI}}} \quad (\text{leaves})$$

$$\text{MR}_i = \max(0, C_{0,i}(\text{MR}_{\text{slope}} \times T_i + \text{MR}_{\text{offset}})) \quad (\text{A15})$$

$$\times B_i \quad (\text{other pools})$$

where $c_{0,i}$ is a coefficient specific to each biomass pool.

Growth respiration (GR)

Growth respiration GR is computed as a fraction K_{GR} of the difference between assimilation inputs and maintenance respiration outputs to plant biomass during 1 day:

$$\text{GR} = K_{\text{GR}} \times \max(B_a - \Delta t \times \sum R_{m,i}, 0.2 \times B_a), \quad (\text{A16})$$

where B_a is the total biomass, and Δt the time step of 1 day.

Heterotrophic respiration (HR)

Processes controlling the decomposition of litter, soil organic matter, and subsequent heterotrophic respiration (R_h) losses of CO_2 to the atmosphere are similar to those described in Parton et al. (1988) and popular amongst biosphere modelers. Soil litter of the forest floor is partitioned into four soil carbon pools (structural/metabolic litter above/below ground), with structural and metabolic pools characterized by different turnover times. Soil organic matter is distributed among three soil carbon pools of increasing turnover (active, passive and slow). The evolution of each of these seven soil carbon pools is governed by a first-order linear differential equation, where pool-specific turnovers have soil moisture ($f_{H,s}$) and soil temperature dependencies $f_{T,s}$ (Eq. A18). To account for the impact of site history on carbon pools, we scale the total R_h flux by the parameter K_{soilC} :

$$\text{HR} = K_{\text{soilC}} \sum_s \frac{\alpha_s}{\tau_s} \times f_{H,s} \times f_{T,s} \times B_s, \quad (\text{A17})$$

where α_s , τ_s and B_s are, respectively, a pool-specific coefficient partitioning HR into pools (Parton et al., 1988), a pool-specific residence time, and the size of the carbon pool s .

The temperature dependency of above-/below-ground pool respirations is a classical Q_{10} function of surface/litter decomposition temperatures $T_{s, \text{litter}}$:

$$f_{T, s, \text{litter}} = \min(1, Q_{10}^{\frac{T_{s, \text{litter}} - 30}{10}}) \quad (\text{A18})$$

The effect of soil temperature on the litter decomposition is assumed to be correlated with an exponential profile of the decomposers that is parameterized by a scaling depth Z_{decomp} . The effective temperature of litter decomposition T_{litter} is then

$$T_{\text{litter}} = \frac{\int_0^{Z_{\text{litter}}} T_{\text{soil}}(z) e^{-\frac{z}{Z_{\text{decomp}}}} dz}{1 - e^{-\frac{Z_{\text{litter}}}{Z_{\text{decomp}}}}}, \quad (\text{A19})$$

where Z_{litter} is the litter depth.

The soil or litter moisture dependencies $f_{H, s, \text{litter}}$ of the above-/below-ground respirations of the soil or the litter are quadratic functions that represent the slowdown of respiration for too dry or too wet soils/litters:

$$f_{H, \text{soil, litter}} = \max(\text{HR}_{H \text{min}}, \min(1, \text{HR}_{H \text{a}} \times H_{\text{soil, litter}}^2 + \text{HR}_{H \text{b}} \times H_{\text{soil, litter}} + \text{HR}_{H \text{c}})) \quad (\text{A20})$$

where $H_{s, \text{litter}}$ are the effective decomposition humidities of the above-ground soil/litter pools.

The effective decomposition humidity of the litter H_{litter} also represents the depth integration of the litter humidity H_1 convoluted to an exponential profile of the decomposers:

$$H_{\text{litter}} = \frac{\int_0^{Z_{\text{litter}}} H_1(z) e^{-\frac{z}{Z_{\text{decomp}}}} dz}{1 - e^{-\frac{Z_{\text{litter}}}{Z_{\text{decomp}}}}} \quad (\text{A21})$$

The litter humidity $H_1(z)$ is an exponential profile of the height of the dry reservoir h_{dry} of the double-bucket hydrological scheme (Choisnel, 1977):

$$H_1(z) = e^{-\frac{h_{\text{dry}}}{Z_{\text{crit_litter}}}}, \quad (\text{A22})$$

where the parameter $Z_{\text{crit_litter}}$ is a scaling depth.

Energy Balance

The energy budget calculation considers that soil and vegetation form a single medium characterized by a common surface temperature T_s . The energy balance is expressed by

$$R_{\text{LW}}^i + (1 - K_{\text{albedo_veg}} \times \text{albedo}_{\text{veg}} - \text{albedo}_{\text{soil, snow, dead leaves}}) \times R_{\text{SW}}^i - \epsilon \sigma T_s^4 = \text{LE} + H + G, \quad (\text{A23})$$

where R_{LW}^i , R_{SW}^i , ϵ and σ are, respectively, the longwave and shortwave incoming radiation, the emissivity and the Stefan–Boltzmann constant. LE, H and G are the latent, sensible and

ground heat fluxes. In ORCHIDEE, shortwave incoming radiation can be reflected by vegetation, soil, dead leaves on the ground and snow. The most important fraction of reflected radiation is determined by the albedo of the vegetation. We scale this fraction by the parameter $K_{\text{albedo_veg}}$.

Latent heat flux (LE)

The latent heat flux is computed as the sum of snow sublimation E_{snow} , soil evaporation E_{soil} , plant evapotranspiration ET and evaporation of water intercepted by foliage $E_{\text{intercept}}$:

$$LE = E_{\text{snow}} + E_{\text{soil}} + ET + E_{\text{intercept}} \quad (\text{A24})$$

The most important fluxes in the Hesse forest are ET and E_{soil} . ET is largely predominant during the growing season whereas the main component of LE during winter is E_{soil} . Each of the LE fluxes is linearly related to the gradient of specific humidity between the evaporating surface, equal to the saturation-specific humidity of the air at the surface temperature ($q_{\text{sat}}(T_s)$) and the air overlying the canopy (q_{air}), the latter being an input forcing. The aerodynamic resistance r_a (Eq. A13) intervenes in the calculation of all LE components, as illustrated for plant transpiration ET in Eq. A25 and for soil evaporation in Eq. A27. The value of r_a mediates the transfer of all scalars from their emitting surface up to the top of the canopy.

Concerning the plant evapotranspiration ET, stomatal responses create a resistance r_c to evaporation processes in addition to the aerodynamic resistance:

$$ET \propto \frac{q_{\text{sat}}(T_s) - q_{\text{air}}}{r_a + r_c} \quad (\text{A25})$$

r_c is the inverse of the canopy conductance g_c (Eq. A12).

For soil evaporation, we introduce a soil resistance to evaporation r_{soil} that is proportional to the dry soil height r_{soil} :

$$r_{\text{soil}} = K_{\text{rsoil}} \times h_{\text{dry}} \quad (\text{A26})$$

and

$$E_{\text{soil}} \propto \frac{q_{\text{sat}}(T_s) - q_{\text{air}}}{r_a + r_{\text{soil}}}. \quad (\text{A27})$$

Leaf area index (LAI)

In ORCHIDEE, LAI is proportional to the leaf biomass (B_l):

$$LAI = SLA \times B_l. \quad (\text{A28})$$

The specific leaf area, SLA, is a parameter specific to each PFT.

When increasing, LAI cannot exceed an upper limit, LAI_{MAX} , which is specific to each PFT as well.

Onset and termination of the growing season

Leaf onset and leaf senescence are fully treated in a prognostic way.

The leaf onset modelling is based on the concept of growing degree days (g) (Botta et al., 2000), which is a way of assessing if the dormant season has been long enough and if the plant has stored enough heat during spring. From mid-winter, when weekly mean temperatures exceeds monthly mean temperature, the value of g is updated the days whom daily temperature T_d is over a threshold temperature T_c :

$$g \leftarrow g + (T_d - T_c)\Delta t \text{ if } T_d > T_c, \quad (\text{A29})$$

where Δt represents the time step of the STOMATE model (1 day in this study), and $T_c = 12^\circ\text{C}$.

For broadleaf summer green trees, biomass starts to be allocated to leaves when g exceeds $g_c(n)$ a threshold function of the number n of chilling days (days with mean temperature below T_c):

$$g_c(n) = K_{\text{pheno_crit}}(ae^{-bn} - c) \quad (\text{A30})$$

where a , b and c are PFT-dependent parameters.

To create the initial foliage, carbon is taken from a carbohydrate reserve until LAI reaches a threshold value LAI_{happy} proportional to the maximum value LAI_{MAX} :

$$B_{\text{tree} \rightarrow \text{leaf}} = \frac{LAI_{\text{happy}}}{LAI_{\text{MAX}}} \times \frac{\Delta t}{\tau_{\text{leafinit}}} \text{ if } LAI < LAI_{\text{happy}} \quad (\text{A31})$$

$$LAI_{\text{happy}} = K_{LAI_{\text{happy}}} \times LAI_{\text{MAX}} \quad (\text{A32})$$

where τ_{leafinit} is the time to attain the initial foliage using the carbohydrate reserve and $B_{\text{tree} \rightarrow \text{leaf}}$ the biomass transferred at each time step from this reserve to the leaves.

For deciduous forests, leaf senescence is triggered when the weekly mean temperature goes below T_{sen} :

$$T_{\text{sen}} = c_{T_{\text{sen}}} + b_{T_{\text{sen}}}T_1 + a_{T_{\text{sen}}}T_1^2, \quad (\text{A33})$$

where T_1 is the annual mean temperature.

A fraction of the leaves ($\Delta B_{\text{loss,age}}$) is lost at every time step as a function of leaf age:

$$\Delta B_{\text{loss,age}} = B_{\text{leaf}} \min(0.99, \frac{\Delta t}{L_{\text{age_crit}}} (\frac{\text{LeafAge}}{L_{\text{age_crit}}})^4) \quad (\text{A34})$$

Acknowledgements. The post-doc program of D. Santaren has been funded by the Swiss Federal Institute of Technology, Zurich (ETH Zurich). The authors thank ANR project PREVASSEMBLE (ANR-08-COSI-012) for financial support and F. Chevallier, N. Vuichard and N. Viovy for fruitful general discussions. Computations were performed thanks to the computer team of the LSCE.

Edited by: M. Williams

References

- Aubinet, M., Grelle, A., Ibrom, A. E. A., Rannik, Ü., Moncrieff, J., Foken, T., Kowalski, A., Martin, P., Berbigier, P., Bernhofer, C., Clement, R., Elbers, J., Granier, A., Grünwald, T., Morgenstern, K., Pilegaard, K., Rebmann, C., Snijders, W., Valentini, R., and Vesala, T.: Estimates of the annual net carbon and water exchange of forests: the EUROFLUX methodology, *Advances in Ecol. Res.*, 30, 113–175, 1999.
- Baldocchi, D., Falge, E., Gu, L., Olson, R., Hollinger, D., Running, S., Anthoni, P., Bernhofer, C., Davis, K., Evans, R., Fuentes, J., Goldstein, A., Katul, G., Law, B., Lee, X., Malhi, Y., Meyers, T., Munger, W., Oechel, W., Paw, K. T. U., Pilegaard, K., Schmid, H. P., and Valentini, R.: FLUXNET: a new tool to study the temporal and spatial variability of ecosystem-scale carbon dioxide, water vapor, and energy flux densities, *B. Am. Meteorol. Soc.*, 82, 2415–2434, 2001.
- Ball, J. T., Woodrow, I., and Berry, J. A.: A model predicting stomatal conductance and its application to the control of photosynthesis under different environmental conditions, *Prog. Photosyn.*, 221–224, 1987.
- Botta, A., Viovy, N., Ciais, P., Friedlingstein, P., and Monfray, P.: A global prognostic scheme of leaf onset using satellite data, *Glob. Change Biol.*, 6, 709–725, 2000.
- Braswell, B. H., Sacks, W. J., Linder, E., and Schimel, D. S.: Estimating diurnal to annual ecosystem parameters by synthesis of a carbon flux model with eddy covariance net ecosystem exchange observations, *Glob. Change Biol.*, 11, 335–355, 2005.
- Breda, N., Huc, R., Granier, A., and Dreyer, E.: Temperate forest trees and stands under severe drought: a review of ecophysiological responses, adaptation processes and long-term consequences, *Ann. For. Sci.*, 63, 625–644, 2006.
- Byrd, R. H., Lu, P., Nocedal, J., and Zhu, C.: A limited memory algorithm for bound constrained optimization, *SIAM J. Sci. Comput.*, 16, 1190–1208, 1995.
- Cadule, P., Friedlingstein, P., Bopp, L., Sitch, S., Jones, C. D., Ciais, P., Piao, S. L., and Peylin, P.: Benchmarking coupled climate-carbon models against long-term atmospheric CO₂ measurements, *Global Biogeochem. Cy.*, 24, GB2016, doi:10.1029/2009GB003556, 2010.
- Carvalhais, N., Reichstein, M., Seixas, J., Collatz, G. J., Pereira, J. A. S., Berbigier, P., Carrara, A., Granier, A., Montagnani, L., Papale, D., Rambal, S., Sanz, M. J., and Valentini, R.: Implications of the carbon cycle steady state assumption for biogeochemical modeling performance and inverse parameter retrieval, *Global Biogeochem. Cy.*, 22, GB2007, doi:10.1029/2007GB003033, 2008.
- Choisnel, E.: Le bilan d'énergie et le bilan hydrique du sol, *Météorologie*, 1977.
- Collatz, G. J., Ribas-Carbo, M., and Berry, J.: Coupled photosynthesis-stomatal conductance model for leaves of C4 plants, *Funct. Plant Biol.*, 19, 519–538, 1992.
- Denman, K. L., Brasseur, G., Chidthaisong, A., Ciais, P., Cox, P. M., Dickinson, R. E., Hauglustaine, D., Heinze, C., Holland, E., Jacob, D., Lohmann, S., Ramachandran, P. L., da Silva, D., Wofsy, S. C., and Zhang, X.: Couplings Between Changes in the Climate System and Biogeochemistry, in: *Climate Change 2007: The Physical Science Basis. Contribution of Working Group I to the Fourth Assessment Report of the Intergovernmental Panel on Climate Change*, edited by: Solomon, S., Qin, D., Manning, M., Chen, Z., Marquis, M., Averyt, K. B., Tignor, M., and Miller, H. L., Cambridge University Press, Cambridge, United Kingdom and New York, NY, USA, 2007.
- Ducoudré, N. I., Laval, K., and Perrier, A.: SECHIBA, a new set of parameterizations of the hydrologic exchanges at the land-atmosphere interface within the LMD atmospheric general circulation model, *J. Climate*, 6, 248–273, 1993.
- Farquhar, G., Caemmerer, S. V., and Berry, J.: A biochemical model of photosynthetic CO₂ assimilation in leaves of C3 species, *Planta*, 149, 78–90, 1980.
- Field, C. B., Jackson, R. B., and Mooney, H. A.: Stomatal responses to increased CO₂: implications from the plant to the global scale, *Plant, Cell and Environment*, 18, 1214–1225, doi:10.1111/j.1365-3040.1995.tb00630.x, 1995.
- Field, C. B., Raupach, R. M.: *The Global Carbon Cycle: Integrating Humans, Climate, and the Natural World*, Island Press, Washington, 2004.
- Fox, A., Williams, M., Richardson, A. D., Cameron, D., Gove, J. H., Quaipe, T., Ricciuto, D., Reichstein, M., Tomelleri, E., Trudinger, C. M., and Van Wijk, M. T.: The REFLEX project: comparing different algorithms and implementations for the inversion of a terrestrial ecosystem model against eddy covariance data, *Agr. Forest Meteorol.*, 149, 1597–1615, doi:10.1016/j.agrformet.2009.05.002, 2009.
- Friedlingstein, P., Cox, P., Betts, R., Bopp, L., Von Bloh, W., Brovkin, V., Cadule, P., Doney, S., Eby, M., Fung, I., Bala, G., John, J., Jones, C., Joos, C., Kato, T., Kawamiya, M., Knorr, W., Lindsay, K., Matthews, H. D., Raddatz, T., Rayner, P., Reick, C., Roeckner, E., Schnitzler, K. G., Schnurr, R., Strassmann, K., Weaver, A. J., Yoshikawa, C., and Zeng, N.: Climate-carbon cycle feedback analysis: results from the C4MIP model intercomparison, *J. Climate*, 19, 3337–3353, 2006.
- Giering, R. and Kaminski, T.: Recipes for adjoint code construction, *ACM T. Math. Softw.*, 24, 437–474, doi:10.1145/293686.293695, 1998.
- Giering, R., Kaminski, T., and Slawig, T.: Generating efficient derivative code with TAF, *Fut. Gen. Comp. Syst.*, 21, 1345–1355, doi:10.1016/j.future.2004.11.003, 2005.
- Goldberg, D.: *Genetic Algorithms in Search, Optimization and Machine Learning*, Addison-Wesley, 1989.
- Granier, A., Breda, N., Longdoz, B., Gross, P., and Ngao, J.: Ten years of fluxes and stand growth in a young beech forest at Hesse, North-eastern France, *Ann. For. Sci.*, 65, 704–704, 2008.
- Groenendijk, M., van der Molen, M. K., and Dolman, A. J.: Seasonal variation in ecosystem parameters derived from FLUXNET

- data, *Biogeosciences Discuss.*, 6, 2863–2912, doi:10.5194/bgd-6-2863-2009, 2009.
- Haupt, R. L. and Haupt, S. E.: *Practical Genetic Algorithms*, John Wiley & Sons, 2004.
- Hui, D., Luo, Y., and Katul, G.: Partitioning interannual variability in net ecosystem exchange between climatic variability and functional change., *Tree Physiol.*, 23, 433–42, 2003.
- Jarvis, P. G.: Scaling processes and problems, *Plant, Cell and Environ.*, 18, 1079–1089, 1995.
- Johnson, I. and Thornley, J.: Temperature dependence of plant and crop process, *Ann. Bot.*, 55, 1–24, 1985.
- Jung, M., Le Maire, G., Zaehle, S., Luyssaert, S., Vetter, M., Churkina, G., Ciais, P., Viovy, N., and Reichstein, M.: Assessing the ability of three land ecosystem models to simulate gross carbon uptake of forests from boreal to Mediterranean climate in Europe, *Biogeosciences*, 4, 647–656, doi:10.5194/bg-4-647-2007, 2007.
- Krinner, G.: A dynamic global vegetation model for studies of the coupled atmosphere-biosphere system, *Global Biogeochem. Cy.*, 19, GB1015, doi:10.1029/2003GB002199, 2005.
- Kuppel, S., Peylin, P., Chevallier, F., Bacour, C., Maignan, F., and Richardson, A. D.: Constraining a global ecosystem model with multi-site eddy-covariance data, *Biogeosciences*, 9, 3757–3776, doi:10.5194/bg-9-3757-2012, 2012.
- Lasslop, G., Reichstein, M., Kattge, J., and Papale, D.: Influences of observation errors in eddy flux data on inverse model parameter estimation, *Biogeosciences*, 5, 1311–1324, doi:10.5194/bg-5-1311-2008, 2008.
- Medlyn, B. E., Robinson, A. P., Clement, R., and McMurtrie, R. E.: On the validation of models of forest CO₂ exchange using eddy covariance data: some perils and pitfalls., *Tree Physiol.*, 25, 839–57, 2005.
- Papale, D., Reichstein, M., Aubinet, M., Canfora, E., Bernhofer, C., Kutsch, W., Longdoz, B., Rambal, S., Valentini, R., Vesala, T., and Yakir, D.: Towards a standardized processing of Net Ecosystem Exchange measured with eddy covariance technique: algorithms and uncertainty estimation, *Biogeosciences*, 3, 571–583, doi:10.5194/bg-3-571-2006, 2006.
- Parton, W. J., Stewart, J. W. B., and Cole, C. V.: Dynamics of C, N, P and S in grassland soils: a model, *Biogeochemistry*, 5, 109–131, doi:10.1007/BF02180320, 1988.
- Press, W. H., Flannery, B. P., Teukolsky, S. A., and Vetterling, W. T.: *Numerical recipes: the art of scientific computing*, Cambridge Univ. Press, Cambridge, 1992.
- Quentin, C., Bigorre, F., Granier, A., Bréda, N., and Tessier, D.: Etude des sols de la forêt de Hesse (Lorraine) Contribution à l'étude du bilan hydrique, *Etude et Gestion des sols*, 8, 279–292, 2001.
- Reichstein, M.: Inverse modeling of seasonal drought effects on canopy CO₂/H₂O exchange in three Mediterranean ecosystems, *J. Geophys. Res.*, 108, 4726, doi:10.1029/2003JD003430, 2003.
- Reichstein, M., Falge, E., Baldocchi, D., Papale, D., Aubinet, M., Berbigier, P., Bernhofer, C., Buchmann, N., Gilmanov, T., Granier, A., Grünwald, T., Havránková, K., Ilvesniemi, H., Janous, D., Knohl, A., Laurila, T., Lohila, A., Loustau, D., Matteucci, G., Meyers, T., Miglietta, F., Ourcival, J.-M., Pumpanen, J., Rambal, S., Rotenberg, E., Sanz, M., Tenhunen, J., Seufert, G., Vaccari, F., Vesala, T., Yakir, D., and Valentini, R.: On the separation of net ecosystem exchange into assimilation and ecosystem respiration: review and improved algorithm, *Glob. Change Biol.*, 11, 1424–1439, 2005.
- Richardson, A. D. and Hollinger, D. Y.: Statistical modeling of ecosystem respiration using eddy covariance data: maximum likelihood parameter estimation, and Monte Carlo simulation of model and parameter uncertainty, applied to three simple models, *Agr. Forest Meteorol.*, 131, 191–208, doi:10.1016/j.agrformet.2005.05.008, 2005.
- Richardson, A. D., Hollinger, D. Y., Aber, J. D., Ollinger, S. V., and Braswell, B. H.: Environmental variation is directly responsible for short- but not long-term variation in forest-atmosphere carbon exchange, *Glob. Change Biol.*, 13, 788–803, doi:10.1111/j.1365-2486.2007.01330.x, 2007.
- Ruimy, A., Kergoat, L., Field, C. B., and Saugier, B.: The use of CO₂ flux measurements in models of the global terrestrial carbon budget, *Glob. Change Biol.*, 2, 287–296, 1996.
- Santaren, D., Peylin, P., Viovy, N., and Ciais, P.: Optimizing a process-based ecosystem model with eddy-covariance flux measurements: a pine forest in southern France, *Global Biogeochem. Cy.*, 21, GB2013, doi:10.1029/2006GB002834, 2007.
- Siqueira, M. B., Katul, G. G., Sampson, D. A., Stoy, P. C., Juang, J.-Y., McCarthy, H. R., and Oren, R.: Multiscale model intercomparisons of CO₂ and H₂O exchange rates in a maturing southeastern US pine forest, *Glob. Change Biol.*, 12, 1189–1207, doi:10.1111/j.1365-2486.2006.01158.x, 2006.
- Spadavecchia, L., Williams, M., and Law, B.: Uncertainty in predictions of forest carbon dynamics: Separating driver error from model error, *Ecol. Appl.*, 21, 1506–1522, 2011.
- Tarantola, A.: *Inverse Problem Theory: Methods for Data Fitting and Parameter Estimation*, Elsevier, 1987.
- Trudinger, C. M., Raupach, M. R., Rayner, P. J., Kattge, J., Liu, Q., Pak, B., Reichstein, M., Renzullo, L., Richardson, A. D., Roxburgh, S. H., Styles, J., Wang, Y. P., Briggs, P., Barrett, D., and Nikolova, S.: OptIC project: An intercomparison of optimization techniques for parameter estimation in terrestrial biogeochemical models, *J. Geophys. Res.*, 112, G02027, doi:10.1029/2006JG000367, 2007.
- Wang, Y.-P., Leuning, R., Cleugh, H. A., and Coppin, P. A.: Parameter estimation in surface exchange models using nonlinear inversion: how many parameters can we estimate and which measurements are most useful?, *Glob. Change Biol.*, 7, 495–510, 2001.
- Wang, Y. P., Baldocchi, D., Leuning, R., Falge, E., and Vesala, T.: Estimating parameters in a land-surface model by applying nonlinear inversion to eddy covariance flux measurements from eight fluxnet sites, *Glob. Change Biol.*, 13, 652–670, 2007.
- Wang, Y.-P., Trudinger, C. M., and Enting, I. G.: A review of applications of model-data fusion to studies of terrestrial carbon fluxes at different scales, *Agr. Forest Meteorol.*, 149, 1829–1842, doi:10.1016/j.agrformet.2009.07.009, 2009.
- Wang, Y. P., Kowalczyk, E., Leuning, R., Abramowitz, G., Raupach, M. R., Pak, B., van Gorsel, E., and Luhar, A.: Diagnosing errors in a land surface model (CABLE) in the time and frequency domains, *J. Geophys. Res.*, 116, G01034, doi:10.1029/2010JG001385, 2011.
- Williams, M., Richardson, A. D., Reichstein, M., Stoy, P. C., Peylin, P., Verbeeck, H., Carvalhais, N., Jung, M., Hollinger, D. Y., Kattge, J., Leuning, R., Luo, Y., Tomelleri, E., Trudinger, C. M., and Wang, Y.-P.: Improving land

- surface models with FLUXNET data, *Biogeosciences*, 6, 1341–1359, doi:10.5194/bg-6-1341-2009, 2009.
- Wilson, K., Goldstein, A., Falge, E., Aubinet, M., Baldocchi, D., Berbigier, P., Bernhofer, C., Ceulemans, R., Dolman, H., Field, C., Grelle, A., Ibrom, A., Law, B. E., Kowalski, A., Meyers, T., Moncrieff, J., Monson, R., Oechel, W., Tenhunen, J., Valentini, R., and Verma, S.: Energy balance closure at FLUXNET sites, *Agr. Forest Meteorol.*, 113, 223–243, 2002.
- Ziehn, T., Scholze, M., and Knorr, W.: On the capability of Monte Carlo and adjoint inversion techniques to derive posterior parameter uncertainties in terrestrial ecosystem models, *Global Biogeochem. Cy.*, 26, GB3025, doi:10.1029/2011GB004185, 2012.